

Comprehensive evaluation of structural geometrical nonlinear solution techniques Part II: Comparing efficiencies of the methods

M. Rezaiee-Pajand*, M. Ghalishooyan and M. Salehi-Ahmadabad

Department of Civil Engineering, School of Engineering, Ferdowsi University of Mashhad, Mashhad, Iran

(Received August 26, 2012, Revised November 6, 2013, Accepted November 9, 2013)

Abstract. In part I of the article, formulation and characteristics of the several well-known structural geometrical nonlinear solution techniques were studied. In the present paper, the efficiencies and capabilities of residual load minimization, normal plane, updated normal plane, cylindrical arc length, work control, residual displacement minimization, generalized displacement control and modified normal flow will be evaluated. To achieve this goal, a comprehensive comparison of these solution methods will be performed. Due to limit page of the article, only the findings of 17 numerical problems, including 2-D and 3-D trusses, 2-D and 3-D frames, and shells, will be presented. Performance of the solution strategies will be considered by doing more than 12500 nonlinear analyses, and conclusions will be drawn based on the outcomes. Most of the mentioned structures have complex nonlinear behavior, including load limit and snap-back points. In this investigation, criteria like number of diverged and complete analyses, the ability of passing load limit and snap-back points, the total number of steps and analysis iterations, the analysis running time and divergence points will be examined. Numerical properties of each problem, like, maximum allowed iteration, divergence tolerance, maximum and minimum size of the load factor, load increment changes and the target point will be selected in such a way that comparison result to be highly reliable. Following this, capabilities and deficiencies of each solution technique will be surveyed in comparison with the other ones, and superior solution schemes will be introduced.

Keywords: nonlinear solution techniques; benchmark problems; path-tracing ability; geometrical nonlinear behavior; comparison study; load limit points; snap-back points

1. Introduction

Nonlinear analysis of the structures is of a great importance among engineers and investigators. Structural analysts have been always looking for a capable solution strategy in order to trace complex nonlinear structural equilibrium paths entirely. In this regard, lots of solution schemes have been developed. It is worth mentioning that researchers have not yet presented a highly robust strategy so that it can completely trace every equilibrium path. Moreover, variety of the available techniques has made it difficult to choose an appropriate solution procedure. In addition, the lack of a comprehensive study on the capabilities of these approaches indicates the importance

*Corresponding author, Professor, E-mail: mrpajand@yahoo.com

of a broad evaluation in this issue.

In the first part of the article, formulations and characteristics of several most widely used procedures in the nonlinear structural analysis were investigated. Incidentally, the methods for determining load factor increment, displacement increment, sign of the load factor increment, choosing the correct root in predictor and corrector step, and the convergence criterion were discussed. In the present paper, performance of nonlinear solution approaches and their analysis aspects are broadly compared by analyzing several benchmark problems with complex nonlinear behavior. To reach this goal, an object oriented finite element program has been prepared by the authors. It is important to note that the basic methods, which were presented in the first part of the article, had very poor numerical performances. Additionally, the three-parameter procedures could not be compared with the other schemes. In fact, they need the defined parameters to run, which are highly depended on the experience of analysts, while the other techniques don't require such parameters. These issues were the reasons to exclude the poor performances of the mentioned nonlinear solvers.

2. Comparison process

For evaluating the capabilities of each solution technique, the numerical performance of their constraint equations are compared with each other. For this purpose, all solution schemes perform the analysis procedure with similar load factors. The number of analysis which the equilibrium path has been successfully traced is computed for each procedure. In this regard, at the beginning of each analysis step, the load factor increment is determined by the user. It should be noted that after selecting the load factor increment, length of the chord in the predictor step is calculated by the following equation

$$L_n = \Delta\lambda_1^1 \|\delta u_1'^1\| \quad (1)$$

Where L_n and $\Delta\lambda_1^1$ denote the chord length of the predictor step and the load factor increment determined by the user, respectively. The parameter $\|\delta u_1'^1\|$ is the displacement increment norm caused by the reference load at the first iteration of the first step. The chord length does not change throughout the analysis and is utilized at the predictor stage of each step. For the subsequent analysis steps, the load factor increment is calculated by coming relationship

$$\Delta\lambda_1^n = \pm \frac{L_n}{\|\delta u_1'^n\|} \quad (2)$$

In the last formula, $\Delta\lambda_1^n$ and $\|\delta u_1'^n\|$ indicate the load increment and displacement increment norm caused by the reference load at the first iteration. These parameters are shown in Fig. 1. It should be noted that chord length of predictor stage is similar for all analysis methods and remains constant up to the end of the analysis in each problem. This factor is specified in properties table of each structure. Then, the achieved point from the predictor step returns to the equilibrium path on the iteration surface based on the constraint equation of the solution strategy. As a result, the numerical performance of constraint equations is compared in returning to the equilibrium path. Several researchers have proposed their solution methods with determining chord length at the

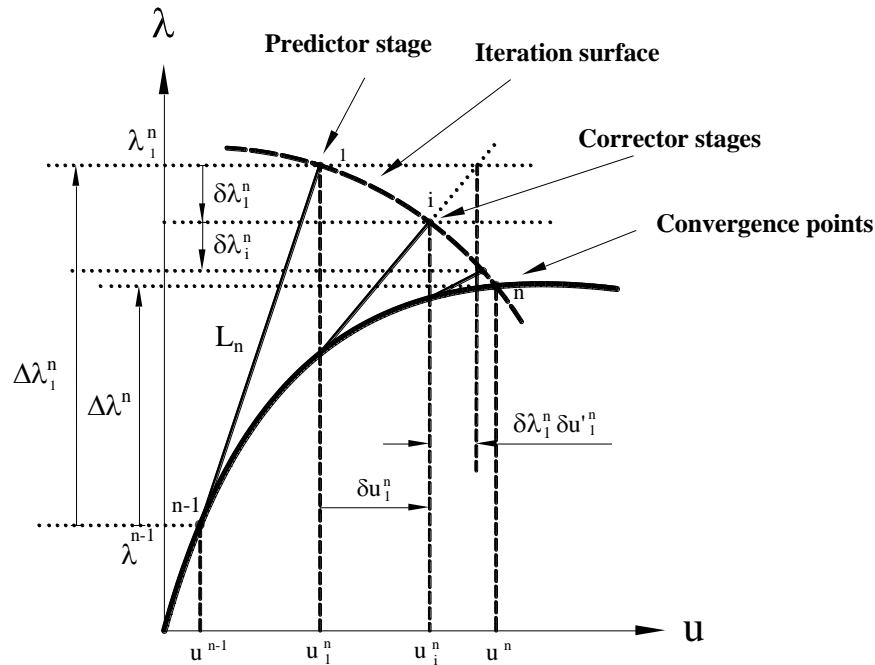


Fig. 1 Nonlinear structural analysis scheme

first iteration. For instance, modified displacement control scheme (Yang and Shieh 1990), and other techniques of determining chord length, like, the current stiffness parameter of Bergan can be stated (Bergan *et al.* 1978). According to these solution tactics, the load factor increments are calculated at the beginning of each analysis step, by the next formulations

$$\Delta\lambda_1^n = \pm\Delta\lambda_1^1(S_p)^\gamma \tag{3}$$

$$\Delta\lambda_1^n = \pm\Delta\lambda_1^1(GSP)^\gamma \tag{4}$$

Where S_p and GSP are current stiffness parameter and Chan's generalized stiffness parameter, respectively. The parameter γ is determined by the analyst. This parameter depends on the degree of structure nonlinear behavior. For implementing similar condition in comparison, the mentioned methods of determining chord length are not utilized in this study.

Benchmark problems are analyzed several times by each method. In this regard, maximum allowed iteration, divergence tolerance, maximum and minimum load factor, the number of analyses and the target point are determined. The target point is defined by expressing a specific load factor or displacement or both. These features are given in a table for each problem. The mentioned parameters are chosen in such a way that the performance capability of the solution techniques can be reliably distinguished. The first load increment is calculated as a specific percentage of the first critical load of the equilibrium path. This calculation has been done by many trial and errors. It should be added that the mentioned factors are similar for all strategies. The solution procedure commences with the minimum arc length and continues to reach the maximum arc length. The results are given in the related tables. The last column of these tables

shows the number of steps, iterations, and the ratio of iterations to calculate steps in one or several complete traces. Convergence criterion used is based on the structural residual load and is formulated by the following inequality

$$R_i^{nT} R_i^n < \varepsilon \quad (5)$$

The parameter R_i^n indicates the residual force vector in the i^{th} iteration of n^{th} analysis step. The factor ε shows the analysis tolerance which is defined by the user. Iterative analysis continues until the convergence criterion is satisfied. If the number of iterations exceeds the maximum allowed value before satisfying the Eq. (5), it is recognized as a diverged analysis. Other kinds of divergence may happen when the points of analysis results go away from the equilibrium path of structure. This is known as the jump failure. In this situation, analysis process does not trace the correct path.

After identifying the number of converged and diverged analyses, location of the divergence points is specified in the figure. Therefore, ability or deficiency of analysis techniques becomes clear in passing snap-through and snap-back points. It should be noted that the examples include a large number of analyses, which make the examining of diverged points difficult. To overcome this shortcoming, instead of indicating all diverged points, divergence ranges are specified, meaning that just the points of beginning and end are drawn in each divergence range. Square points illustrated in the figures show the locations that number of negative diagonal arrays of the stiffness matrix changes. For this purpose, the number of negative diagonal arrays of the stiffness matrix is calculated. When this number is increased or decreased, analysis step is recorded. These are called special points. It is interesting to note that Huang and Atluri (1995) have developed a technique based on the mentioned arrays for tracing post-buckling path of the structures and after bifurcation points.

In this comparison procedure, criteria like the number of successfully converged analyses, ability to pass the limit points, total number of iterations and average number of iterations in each analysis step are examined. The average number of iterations to analysis steps denotes convergence speed of the method in each analysis step. As a result, a comprehensive evaluation is performed on most widely used nonlinear solution approaches. Equilibrium path of the structures is illustrated by the load factor-displacement figures. Vertical and horizontal axes of these figures indicate the size of the reference load factor and displacement, respectively. The normal axis will be rescaled by multiplying in the reference load. The amount of reference loads is specified in each problem.

3. Numerical examples

In this part, some problems are solved by different nonlinear solution strategies, and the results of the analysis are given in the related table. Capability of traversing snap-through and snap-back points, number of iterations and calculated steps are the factors of comparing the solutions. In this section, 17 structures including 2-D and 3-D trusses, 2-D and 3-D frames, and shells are analyzed. This section contains 16 benchmark problems and the one which has been proposed by the authors. For sure, these examples are famous in comparative cases and the more practical ones have been employed by several researchers (Xu *et al.* 2010, Gorgun and Yilmaz 2012, Kim *et al.* 2012). For simplicity, the short form of the methods name is used throughout the article. Table 1

Table 1 Nonlinear solution methods

Row	Analysis method	Short form
1	Residual Load Minimization	RLM
2	Normal Plane	NP
3	Updated Normal Plane	UNP
4	Cylindrical Arc Length	CAL
5	Work Control	WC
6	Residual Displacement Minimization	RDM
7	Generalized Displacement Control	GDC
8	Modified Normal Flow	MNF

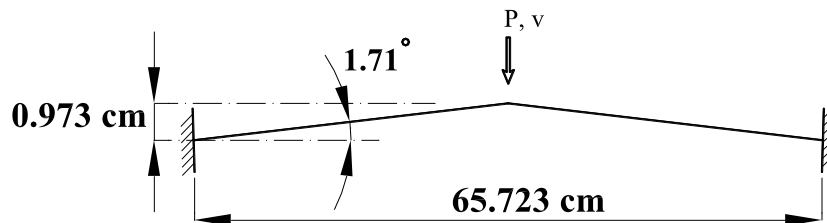


Fig. 2 William Toggle frame

Table 2 Analysis properties of William Toggle frame

Max. of Iteration	Tolerance for Conv.	Arc Length			Target Point	
		Minimum	Increment	Num. of analyses	Load Factor	Displacement
3	1×10^{-8}	0.1	0.005	50	75	-

shows the complete and abbreviation name of the solution techniques.

3.1 Problem one

Two-member frame of Fig. 2 has a span of 65.723 cm (25.875 in), and height of 0.973 cm (0.386 in). This clamped frame was analyzed by Williams (1964), and the result was compared with the experimental observations. Wood and Zienkiewicz (1977) have studied these structures using finite element solution. Axial and flexural rigidity of members are considered to be $EA=8252 \text{ kN}$ ($EA=1855 \text{ klb}$) and $EI=266 \text{ kN.cm}^2$ ($EI=927 \text{ klb.in}^2$), respectively. There is a vertical downward load ($P=1 \text{ N}$) on the top node of the frame. The analysis result for vertical downward displacement of the tip node (v) is shown in Fig. 3. Two elements were used for modeling this structure. Investigators have extensively analyzed this problem for assessing the ability of methods in passing load limit points. Table 2 shows the analysis properties of William Toggle frame.

In Fig. 3, two load limit points can be seen. The findings indicate the failure of Newton-Raphson and modified Newton-Raphson procedures in passing the load limit points. Based on Table 3, the solution techniques have achieved the target point in all analyses. Due to the simple equilibrium path and geometry of the structure and low number of its degrees of freedom, the total number of iterations and analysis steps is equal for all strategies in arc length of 0.215. The details of results are shown in Table 3.

Table 3 Numerical results of William Toggle frame

Solution Techniques	Number of Analyses	Number of Complete Tracing	Number of Failures	Number of Jumps	Complete Tracing (%)	Steps- Iteration (Ratio)
RLM	50	50	0	0	100	11- 12 (1.091)
NP	50	50	0	0	100	11- 12 (1.091)
UNP	50	50	0	0	100	11- 12 (1.091)
CAL	50	50	0	0	100	11- 12 (1.091)
WC	50	50	0	0	100	11- 12 (1.091)
RDM	50	50	0	0	100	11- 12 (1.091)
GDC	50	50	0	0	100	11- 12 (1.091)
MNF	50	50	0	0	100	11- 12 (1.091)

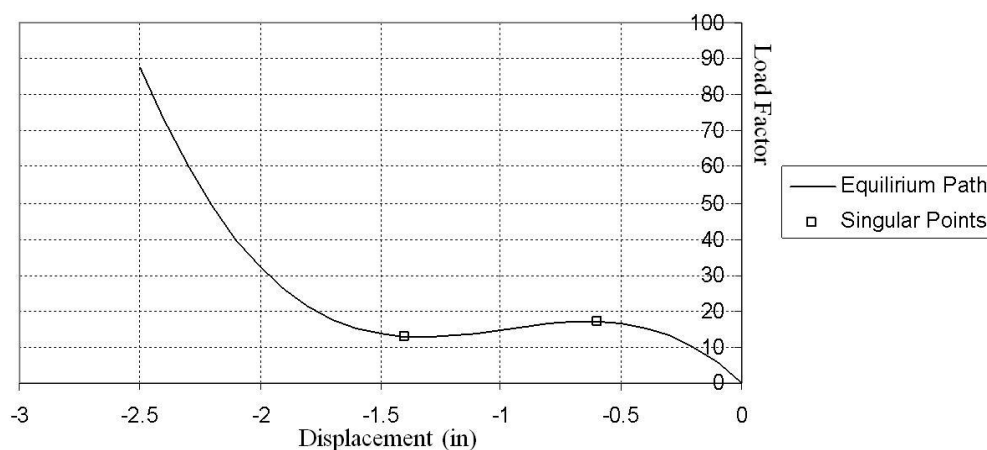


Fig. 3 Equilibrium path of William Toggle frame

Table 4 Analysis properties of 12-member truss

Max. of Iteration	Tolerance for Conv.	Arc Length			Target Point	
		Minimum	Increment	Num. of analyses	Load Factor	Displacement
3	1×10^{-5}	1	0.05	80	0.2	-

3.2 Problem two

Fig. 4 presents a truss with 12 members and 9 nodes. Size of the members is shown in this figure. There are three downward vertical loads ($P=1 N$) on the nodes 1, 2, and 3. Nodes indicated with the circle are pinned supports at the height of zero ($Z=0$), and nodes 1, 2, and 3 are at the height of $Z=-35.355$ cm. Members cross-section area and Young's modulus of elasticity are $A=10 \text{ cm}^2$ and $E=1 \times 10^6 Pa$, respectively. Fig. 5 shows the load factor-deflection curve for node 1 in W (Z) direction. The analysis properties of this truss are presented in Table 4. In 1994, this problem was solved by Yang and kuo (1994).

Table 5 shows the total number of iterations and analysis steps for arc length of 1 to 4.95. Based on the results, generalized displacement control technique has the least number of iterations and analysis steps. Number of iterations in this approach has a huge difference with other methods.

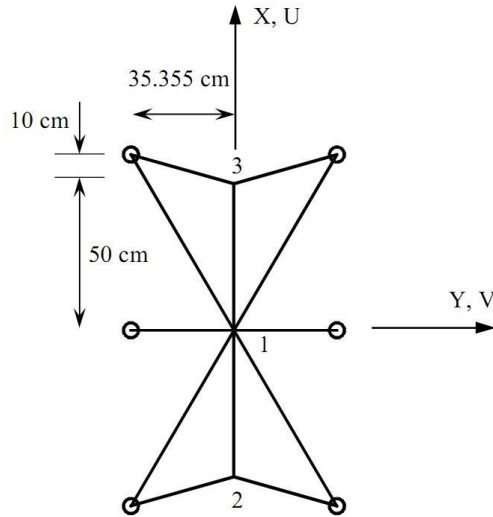


Fig. 4 12-member truss

Table 5 Numerical results of 12-member truss

Solution Techniques	Number of Analyses	Number of Complete Tracing	Number of Failures	Number of Jumps	Complete Tracing (%)	Steps- Iteration (Ratio)
RLM	80	0	80	0	0	Failed
NP	80	80	0	0	100	12591- 15446 (1.227)
UNP	80	80	0	0	100	12591- 15446 (1.227)
CAL	80	80	0	0	100	12601- 15469 (1.228)
WC	80	0	80	0	0	Failed
RDM	80	80	0	0	100	12636- 15523 (1.228)
GDC	80	80	0	0	100	12532- 15403 (1.229)
MNF	80	80	0	0	100	12613- 15463 (1.226)

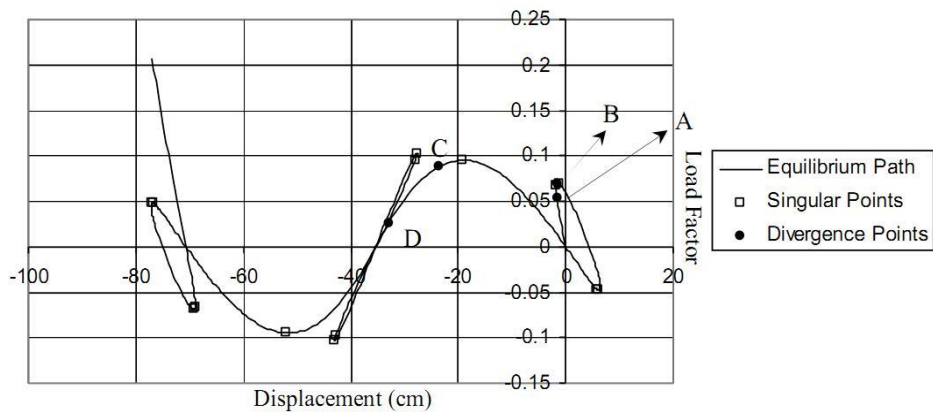


Fig. 5 Equilibrium path of 12-member truss

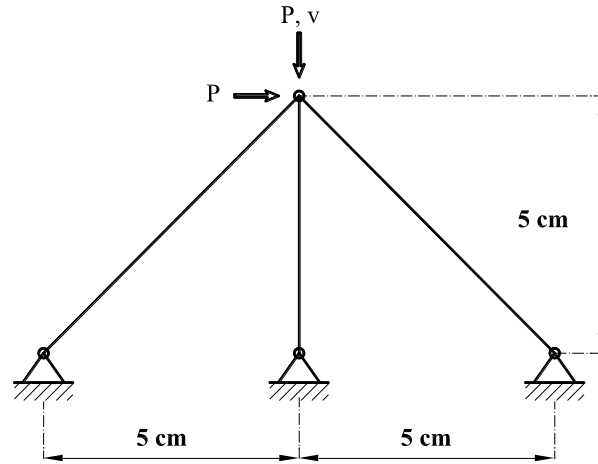


Fig. 6 Three-member truss

Table 6 Analysis properties of three- member truss

Max. of Iteration	Tolerance for Conv.	Arc Length			Target Point	
		Minimum	Increment	Num. of analyses	Load Factor	Displacement
5	1×10^{-4}	0.250	0.015	45	-18.11	-5.9

According to Fig. 5, the equilibrium path of 12-member truss has many snap-back and load limit points. Residual load minimization and constant work control processes diverged in all the 80 analyses. Other methods traced the equilibrium path completely. The approach of residual load minimization was diverged at the first load limit point. This shows the deficiency of this algorithm in passing snap-through points in structures with complex behavior and geometry, and large degrees of freedom. Divergence range of this approach is AB. Constant work control solution also diverged in range CD.

3.3. Problem three

Fig. 6 illustrates a three-member truss, which has 3 pinned supports. This structure has 4 nodes and 2 degrees of freedom. The tip node is subjected to horizontal and vertical point loads with the amount of $P=1000 \text{ N}$. Axial rigidity of members is $AE=2 \times 10^5 \text{ N}$. Fig. 7 shows the load-displacement curve of structure for vertical degree of freedom (v). Bathe and Dvorkin (1983) analyzed a structure like the present problem. Table 6 indicates the analysis properties of three-member truss.

Table 7 indicates that residual displacement minimization and modified normal flow have entirely traced the equilibrium path in all analyses. Constant work control strategy failed in all the solutions. Other results are also shown in this table. In addition, the required number of steps and iterations of generalized displacement control for the arc length of 0.415 was lesser than that of other techniques. On the other hand, residual load minimization procedure has the maximum number of iterations and also the maximum amount of iteration ratio in each step.

Table 7 Numerical results of three-member truss

Solution Techniques	Number of Analyses	Number of Complete Tracing	Number of Failures	Number of Jumps	Complete Tracing (%)	Steps- Iterations (ratio)
RLM	45	31	2	12	68.89	23- 61 (2.652)
NP	45	29	11	5	64.44	22- 52 (2.364)
UNP	45	35	5	5	77.78	22- 52 (2.364)
CAL	45	43	2	0	95.56	22- 52 (2.364)
WC	45	0	45	0	0	Failed
RDM	45	45	0	0	100	23- 54 (2.348)
GDC	45	6	39	0	13.33	19- 48 (2.526)
MNF	45	45	0	0	100	23- 54 (2.348)

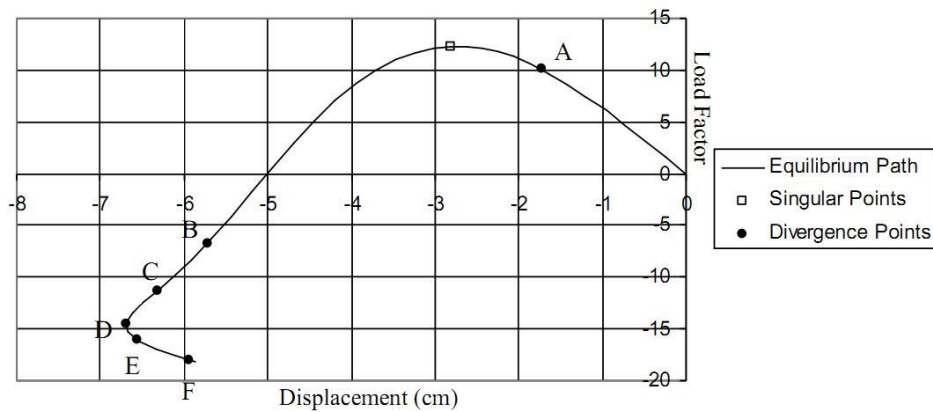


Fig. 7 Equilibrium path of three-member truss

Fig. 7 presents that this structure has load and displacement limit points. Residual load minimization diverged in point A and in the range of EF. Constant work control solution failed before Snap-back point (range BD). Diverged analyses of generalized displacement control are located in BE range. Cylindrical arc length methods, updated normal plane, residual displacement minimization and modified normal flow diverged in DE. Diverged analyses of the normal plane are also in the range of CE.

2.4 Problem four

Several investigators have studied eight-member truss shown in Fig. 8 (Powell and Simons 1981, Feenstra and Schellekens 1991, Geers 1999). Moreover, a similar case has been explored by Bathe and Dvorkin (1983). Fig. 9 shows the load-deflection curve for the displacement u . The analysis properties of this truss are illustrated in Table 8. This problem has several limit points, and it is appropriate for evaluation of the nonlinear solution approaches. There is a horizontal point load $P=100$ kN on the node 1. Axial rigidity of all members is $EA=3 \times 10^6$ N.

According to the 300 performed analyses, cylindrical arc length and updated normal plane techniques have the best outcomes. They traced the structural path completely in all analyses. The modified normal flow, residual load minimization and constant work control diverged in most

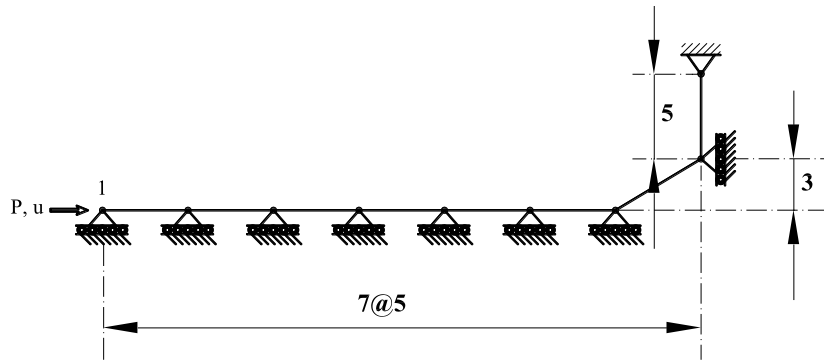


Fig. 8 Eight-member truss

Table 8 Analysis properties of eight-member truss

Max. of Iteration	Tolerance for Conv.	Arc Length			Target Point	
		Minimum	Increment	Num. of analyses	Load Factor	Displacement
5	1×10^{-4}	1	0.01	300	-	16

Table 9 Numerical results of 8-member truss

Solution Techniques	Number of Analyses	Number of Complete Tracing	Number of Failures	Number of Jumps	Complete Tracing (%)	Steps- Iterations (ratio)
RLM	300	1	299	0	0.33	Failed
NP	300	206	94	0	68.67	17- 33 (1.941)
UNP	300	300	0	0	100	17- 33 (1.941)
CAL	300	300	0	0	100	17- 33 (1.941)
WC	300	8	292	0	2.67	Failed
RDM	300	293	7	0	97.67	19- 40 (2.105)
GDC	300	124	176	0	41.11	15- 31 (2.067)
MNF	300	0	300	0	0	Failed

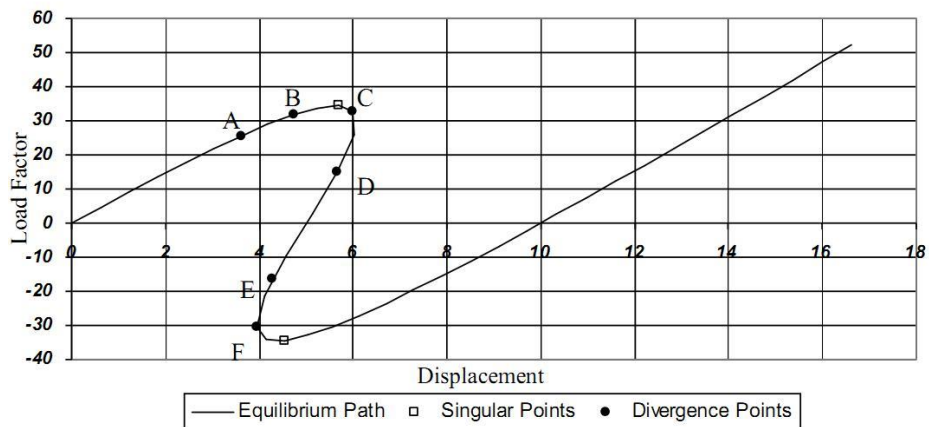


Fig. 9 Equilibrium path of eight-member truss

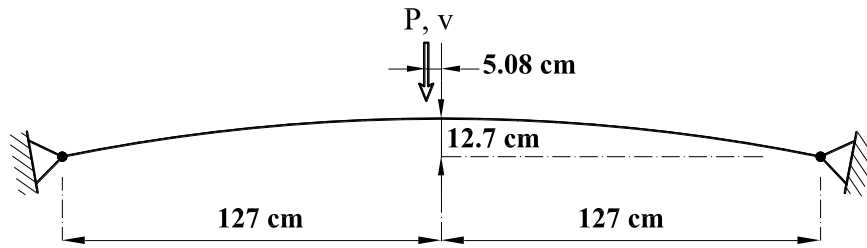


Fig. 10 Shallow arc frame

Table 10 Analysis properties of shallow arc frame

Max. of Iteration	Tolerance for Conv.	Arc Length			Target Point	
		Minimum	Increment	Num. of analyses	Load Factor	Displacement
20	1×10^{-4}	20	0.5	100	-	1000

solutions. Divergence ranges of different techniques are shown in Fig. 9. Based on Table 9, generalized displacement control method has the minimum number of iterations and steps for the arc length of 2.51.

All the analyses of residual load minimization diverged in the range AB. Diverged solutions of the normal plane, constant work control, and modified normal flow are in the BC domain. Approaches of the constant work control and generalized displacement control failed before the snap-back point of C and in the range BD, respectively. So far, the last two examples show deficiency of work control method in tracing snap-back points. Divergent analyses of updated normal plane and residual displacement minimization occurred in the EF domain.

3.5 Problem five

The frame shown in Fig. 10 is subjected to a point load ($P=1\text{ N}$), with eccentricity of $b=5.08\text{ cm}$ ($b=2\text{ in}$). The horizontal length and height of the structure are $L=254\text{ cm}$ ($L=100\text{ in}$) and $h=12.7\text{ cm}$ ($h=5\text{ in}$), respectively. 12 similar elements have been used to model this shallow arc frame. According to the figure, the structure is hinged at its two ends. The nonlinear behavior of this frame for vertical nodal degree of freedom under the load is shown in Fig. 11. Cross-section area, the second moment of area and Young's modulus of elasticity are $A=6.45\text{ cm}^2$ ($A=1\text{ in}^2$), $I=41.62\text{ cm}^4$ ($I=1\text{ in}^4$) and $E=1378\text{ kPa}$ ($E=200\text{ psi}$), respectively. Other related properties are given in Table 10. It should be mentioned that Harrison (1983) analyzed this structure using the discrete element method. Other researchers have also studied this arc frame (Yang and Kuo 1994, Rezaiee-Pajand *et al.* 2009, Clarke and Hancock 1990).

Fig. 11 indicates the complex behavior of the shallow arc with Snap-through and Snap-back points. Nonlinear analysis techniques are assessed by doing 100 analyses. Among these, residual displacement minimization has the best performance with 97 successful tracing. The constant work control and residual load displacement minimization solutions didn't achieve the target point in any analyses. The results are given in Table 11. The normal plane scheme has the minimum number of iterations for the arc length of 46.5. Furthermore, this technique has the least ratio of total iterations to total analysis steps.

Table 11 Numerical results of shallow arc frame

Solution Techniques	Number of Analyses	Number of Convergence	Number of Failures	Number of Jumps	Complete Tracing (%)	Steps- Iterations (ratio)
RLM	100	0	100	0	0	Failed
NP	100	73	27	0	73	116- 406 (3.500)
UNP	100	58	36	6	58	116- 410 (3.534)
CAL	100	75	25	0	75	117- 414 (3.538)
WC	100	0	100	0	0	Failed
RDM	100	94	6	0	94	117- 417 (3.564)
GDC	100	17	83	0	17	Failed
MNF	100	0	100	0	0	Failed

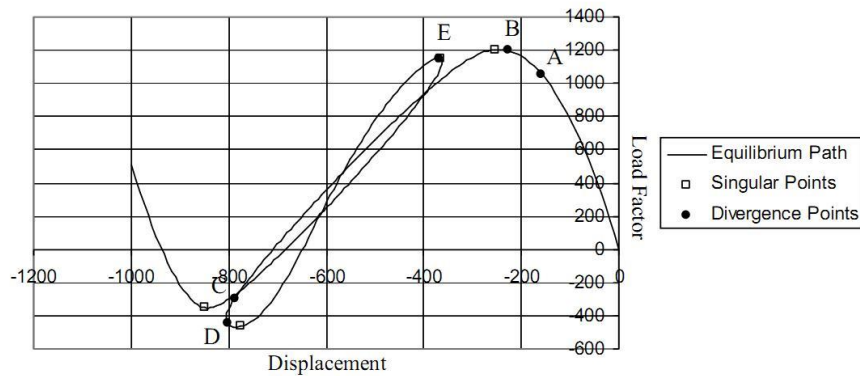


Fig. 11 Equilibrium path of shallow arc frame

Fig. 11 shows the equilibrium path of the shallow arc frame. The residual load minimization and constant work control methods diverged in AB and CD domain, respectively. As it was mentioned previously, the preceding procedures are incapable of passing load limit and snap-back point. Diverged analyses of the normal plane and generalized displacement control happened in E and D. Divergences of updated normal plane, cylindrical arc length, residual displacement minimization, and modified normal flow occurred in point D. Sharp snap-back points mostly specify the diverged points of the normal plane and updated normal plane.

3.6 Problem six

The arc frame of Fig. 12 pinned at both ends has been examined by Harrison (1983). Yang *et al.* (1990, 1994) have also studied this structure. The arc radius is $R=127$ cm ($R=50$ in). The second moment of area and Young's modulus of elasticity are $E=1378$ kPa ($E=200$ psi) and $I=41.62$ cm⁴ ($I=1$ in⁴), respectively. Cross-section area of the member is also considered to be $A=64.5$ cm² ($A=10$ in²). In this example, the structure is divided into 26 equal elements. Referring to Fig. 12, the arc frame is subjected to a vertical point load ($P=1$ N) with eccentricity of $b=7.98$ cm ($b=3.14$ in). The load-deflection curve for the vertical direction of the top node is considered. Fig. 13 shows the result of this analysis. Analysis properties of the deep arc frame are included in Table 12.

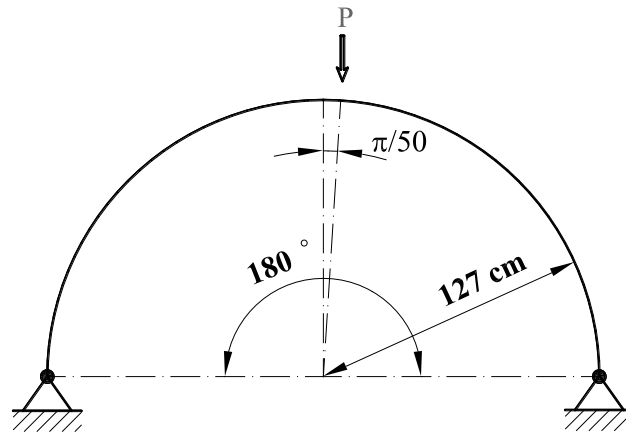


Fig. 12 Deep arc frame

Table 12 Analysis properties of deep arc frame

Max. of Iteration	Tolerance for Conv.	Arc Length			Target Point	
		Minimum	Increment	Num. of analyses	Load Factor	Displacement
8	1×10^{-4}	5	0.1	40	1.75	-22.6

Table 13 Numerical results of deep arc frame

Solution Techniques	Number of Analyses	Number of Complete Tracing	Number of Failures	Number of Jumps	Complete Tracing (%)	Steps- Iterations (ratio)
RLM	40	0	40	0	0	Failed
NP	40	27	13	0	67.5	3987- 9745 (2.444)
UNP	40	21	19	0	52.5	3987- 9775 (2.452)
CAL	40	26	14	0	65	3994- 9778 (2.448)
WC	40	0	40	0	0	Failed
RDM	40	27	13	0	67.5	4010- 9884 (2.465)
GDC	40	2	38	0	5	Failed
MNF	40	0	40	0	0	Failed

The structural equilibrium path illustrated in Fig. 13 has several snap-through and snap-back points. Based on Table 13, the displacement minimization scheme has the best result by completely tracing the equilibrium path in 67.5 % of analyses. The residual load minimization, constant work control, and modified normal flow diverged in all analyses. In the meantime, the normal plane has the minimum number of iterations and ratio of total iterations to analysis steps for the arc lengths of 5 to 6.5.

Fig. 13 represents the equilibrium path of this structure. Like what was found in previous problems, all the analyses of residual load minimization and constant work control methods diverged in the ranges of AB and CD, respectively. Some of the analyses of generalized displacement control algorithm diverged in the DE region, and the others diverged in point F. Divergent solutions of the normal plane, updated normal plane, cylindrical arc length and modified normal flow happened at the sharp snap-back point of F.

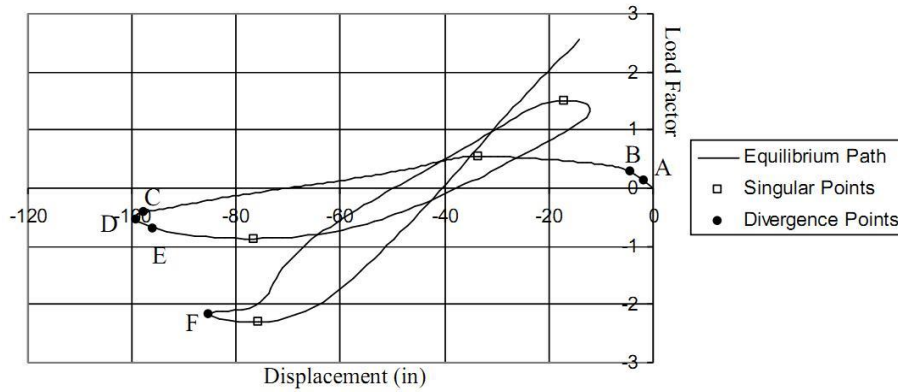


Fig. 13 Equilibrium path of deep arc frame

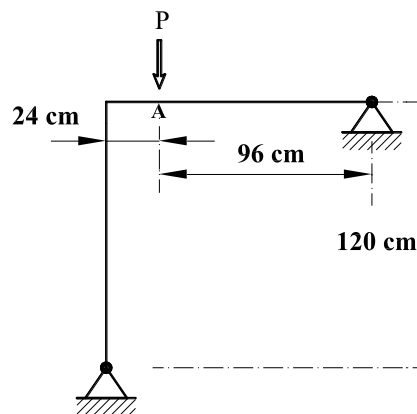


Fig. 14 Lee frame

3.7 Problem seven

Lee *et al.* (1968) have numerically examined nonlinear behavior of the frame shown in Fig. 14. There is a downward vertical point load ($P=100$) in point A. Analysis of this structure is performed by dividing it into 20 equal frame members. The result of the analysis is drawn in Fig. 15 for horizontal direction of point A. The cross-section area, Young's modulus of elasticity and the second moment of area of the members are $A=6$, $E=7.2 \times 10^{-6}$ and $I=2$, respectively. Geometry, loading, and the positions of supports of this frame are shown in Fig. 14. Also, Table 14 shows the analysis properties of Lee frame. It is worth mentioning that this structure has been studied by many researchers (Schweizerhof and Wriggers 1986, Simo and Vu-Quoc 1986, Kuo Mo Hsiao and Fang Yu Hou 1987, Schellekens *et al.* 1992, Chen and Blandford 1993, Cardona and Huespe 1998, Geers 1999, Paulino *et al.* 1999).

Referring to Fig. 15, the equilibrium path has a few limit points and extreme stiffening at the end. Based on Table 15, the normal plane and generalized displacement control methods have traced the path completely in all analyses. Analysis findings and the constraint equation of residual

Table 14 Analysis properties of Lee frame

Max. of Iteration	Tolerance for Conv.	Arc Length			Target Point	
		Minimum	Increment	Num. of analyses	Load Factor	Displacement
13	1×10^{-4}	5	0.05	180	29	89.3

Table 15 Numerical results of Lee frame

Solution Techniques	Number of Analyses	Number of Complete Tracing	Number of Failures	Number of Jumps	Complete Tracing (%)	Steps- Iterations (ratio)
RLM	180	0	41	139	0	Failed
NP	180	180	0	0	100	7974- 23748 (2.978)
UNP	180	153	27	0	85	7971- 23898 (2.998)
CAL	180	165	15	0	91.67	7991- 23948 (2.997)
WC	180	0	111	69	0	Failed
RDM	180	170	10	0	94.44	8086- 25188 (3.115)
GDC	180	180	0	0	100	7924- 23445 (2.959)
MNF	180	174	6	0	96.67	8022- 23842 (2.972)

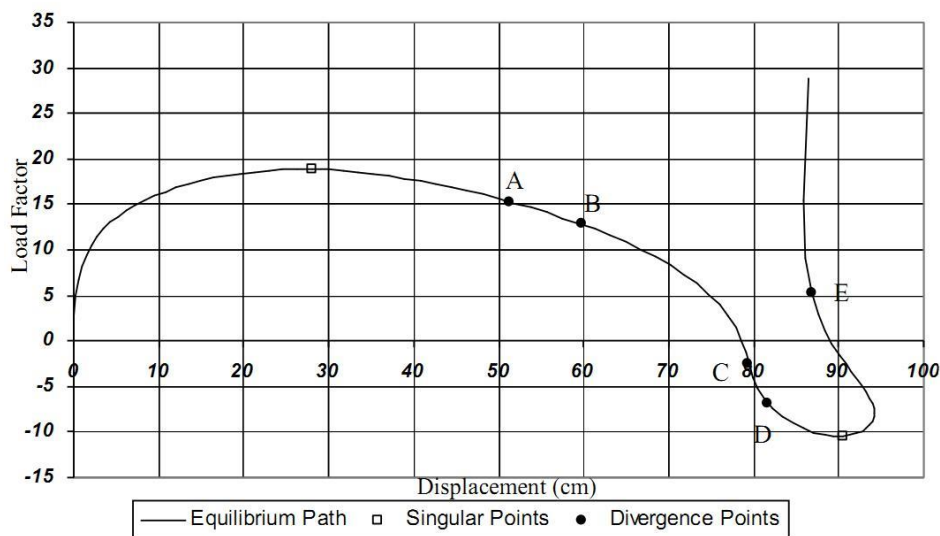


Fig. 15 Equilibrium path of Lee frame

displacement minimization indicate that this process may face difficulties in analyzing structures with extreme stiffening behavior. On the other hand, the generalized displacement control method has a better performance in such structures. The total number of iterations and analysis steps in arc lengths of 5 to 11.7 has been shown in Table 15.

The residual load minimization method diverged in first steps of the analysis. The constant work control strategy failed in AB region. The techniques of Normal plane, updated normal plane, cylindrical arc length and modified normal flow also diverged in range of CD. Diverged analyses of residual displacement minimization method occurred in point E.

3.8 Problem eight

Dome truss of Fig. 16 has 61 nodes and 156 members. The ratio of external span size to the height is 10. The dome is subjected to a downward point load of 1000 N at the apex. All the members of this structure have identical properties. The cross-section area, Young's modulus of elasticity, and the second moment of area of the members are $A=6.5 \text{ cm}^2$, $E=6895 \text{ kN/cm}^2$ and $I=1 \text{ cm}^4$, respectively. External edge nodes of the dome, which were shown by empty circles, are pinned support. The geometry of truss has the following formulation

$$x^2 + y^2 + (z + 7.2)^2 = 60.48 \quad (6)$$

This problem has been so far analyzed by many researchers (Noor and Peters 1983, Meek and Loganathan 1989, Loganathan 1989, Meek and Xue 1998). Ramesh and Krishnamoorthy (1994) have studied it using dynamic relaxation method. Furthermore, Thai and Kim (2009) investigated this structure using the generalized displacement control procedure. Nonlinear analysis response of the geodesic dome truss for the top node and downward degree of freedom is presented in Fig. 17. Analysis properties of geodesic dome truss are presented in Table 14.

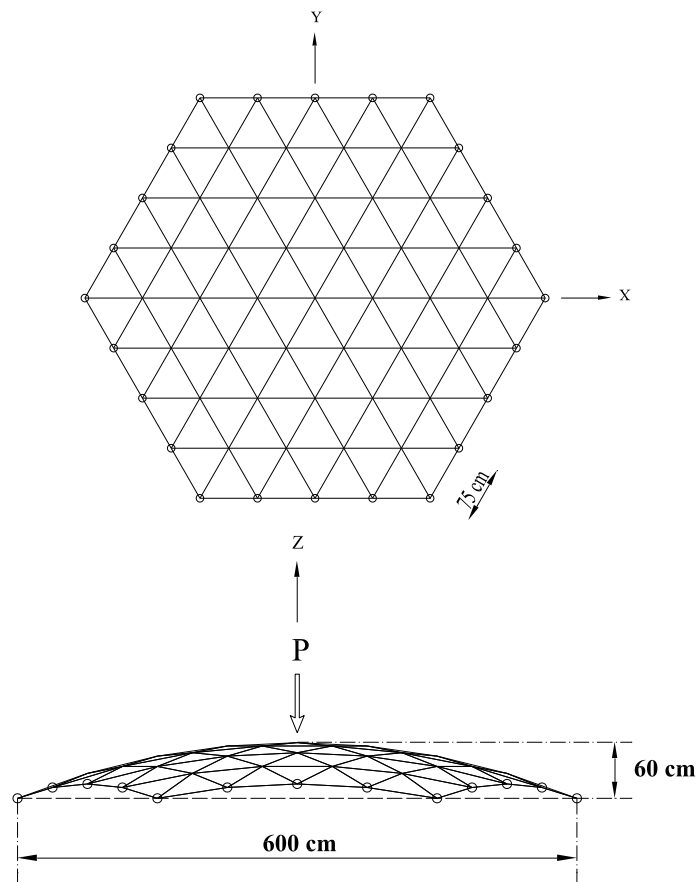


Fig. 16 Geodesic dome truss

Table 16 Analysis properties of geodesic dome truss

Max. of Iteration	Tolerance for Conv.	Arc Length			Target Point	
		Minimum	Increment	Num. of analyses	Load Factor	Displacement
8	1×10^{-4}	0.005	0.0005	30	-	0.3

Table 17 Numerical results of geodesic dome truss

Solution Techniques	Number of Analyses	Number of Complete Tracing	Number of Failures	Number of Jumps	Complete Tracing (%)	Steps- Iterations (ratio)
RLM	30	0	23	7	0	Failed
NP	30	15	15	0	50	1347- 3146 (2.336)
UNP	30	30	0	0	100	1360- 3159 (2.323)
CAL	30	28	2	0	93	1366- 3174 (2.324)
WC	30	0	30	0	0	Failed
RDM	30	30	0	0	100	1376- 3211 (2.334)
GDC	30	0	30	0	0	Failed
MNF	30	30	0	0	100	1369- 3184 (2.326)

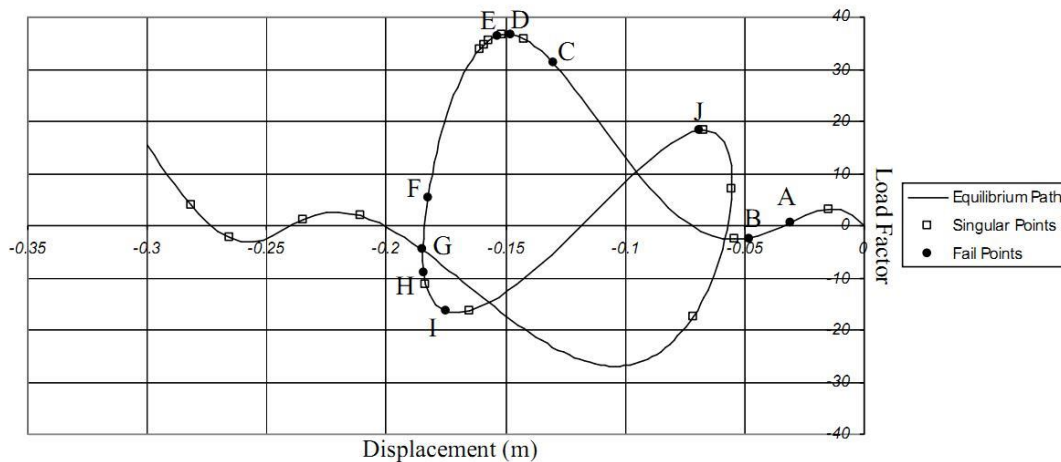


Fig. 17 Equilibrium path of geodesic dome truss

The work control, residual load minimization, and generalized displacement control methods were not able to trace the load-deflection curve completely. The updated normal plane, residual displacement minimization, and modified normal flow had the superior performance. They achieved the target point in all analyses. Table 17 shows these results. The normal plane and modified normal plane strategies have the minimum number of iterations and analysis steps to reach the target point for the arc lengths of 0.006 to 0.011.

Referring to Fig. 17, divergence points of the residual load minimization are in AB and CD regions. Diverged analyses of cylindrical arc length occurred in point E. The range of FG contains constant work control diverged points. The normal plane and generalized displacement control techniques diverged in the HI domain. Some other diverged analyses of the generalized displacement control happened in point J.

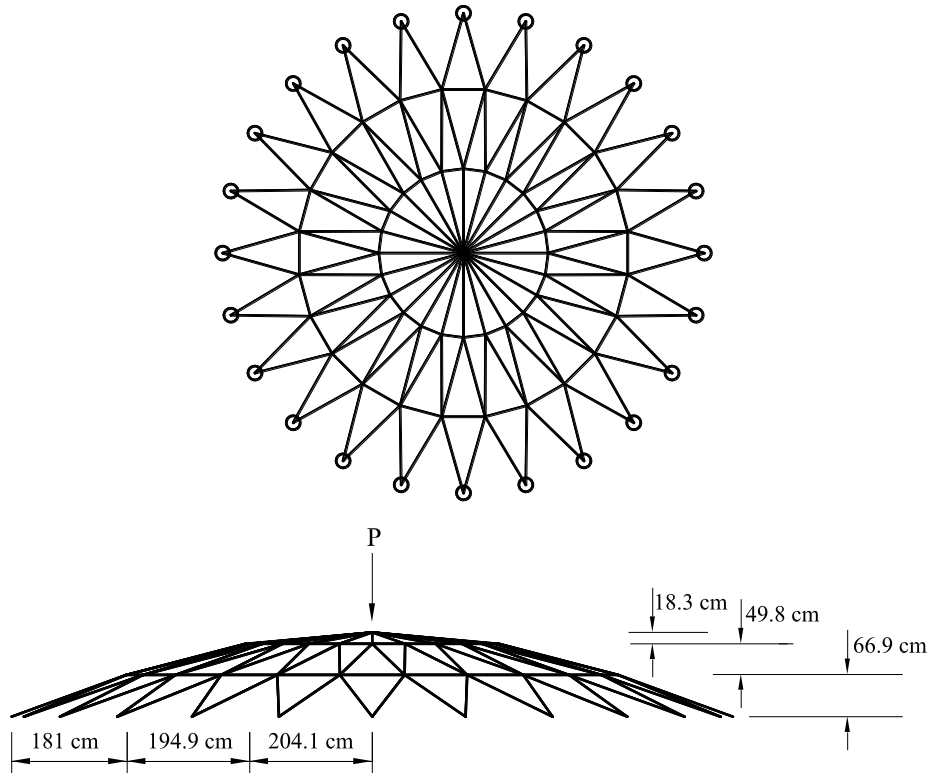


Fig. 18 Circle dome truss

Table 18 Analysis properties of circle dome truss

Max. of Iteration	Tolerance for Conv.	Arc Length			Target Point	
		Minimum	Increment	Num. of analyses	Load Factor	Displacement
4	1×10^{-5}	1	0.025	120	-4.5	-80

3.9 Problem nine

Dome truss illustrated in Fig. 18 has 168 members and 73 nodes. Cross-section area of all structure members is $A=50.431 \text{ cm}^2$. The modulus of elasticity and the second moment of area of the dome members are $E=2.04 \times 10^4 \text{ kN/cm}^2$ and $I=52.942 \text{ cm}^4$, respectively. The top node of the dome is subjected to a downward vertical point load of 1000 kN. As presented in Fig. 18, all nodes of the largest span of the dome are pinned support. These nodes are shown with empty circles. Equilibrium path of circle dome truss is illustrated in Fig. 19 for the top node and downward degree of freedom. Analysis properties of circle dome truss are given in Table 18. It should be added that this problem has been investigated by many researchers (Powell and Simons 1981, Yang *et al.* 1997, Saffari *et al.* 2008, Rezaiee-Pajand *et al.* 2009, Thai and Kim 2009).

Table 19 denotes that the residual displacement minimization and Crisfield cylindrical arc length technique had the best tracing results. The residual load minimization, work control, generalized displacement control, and modified normal flow strategies failed in all the analyses.

Table 19 Numerical results of circle dome truss

Solution Techniques	Number of Analyses	Number of Complete Tracing	Number of Failures	Number of Jumps	Complete Tracing (%)	Steps- Iterations (ratio)
RLM	120	0	120	0	0	Failed
NP	120	71	49	0	59.17	6286- 7794 (1.240)
UNP	120	112	8	0	93.33	6286- 7791 (1.239)
CAL	120	120	0	0	100	6292- 7799 (1.240)
WC	120	0	120	0	0	Failed
RDM	120	120	0	0	100	6295- 7814 (1.241)
GDC	120	22	98	0	18.33	6274- 7803 (1.244)
MFP	120	0	120	0	0	Failed

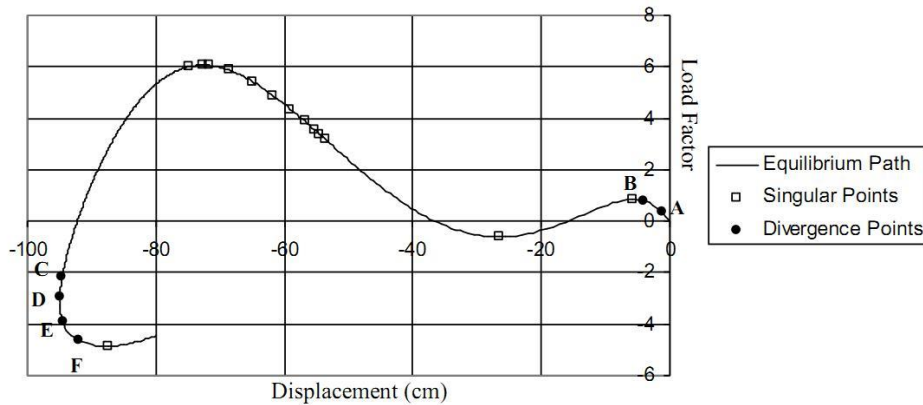


Fig. 19 Equilibrium path of circle dome truss

The generalized displacement control and updated normal plane have the minimum number of steps and analysis iterations, respectively. The number of steps and iterations is calculated for the arc lengths of 1 to 1.6 except arc lengths of 1.5, 1.55, and 1.575 that some methods diverged.

Referring to Fig. 19, AB and CD regions illustrate the divergence range of residual load minimization and constant work control approaches, respectively. These domains are located before snap-through and snap-back point. The failed analyses of cylindrical arc length, normal plane, updated normal plane, residual displacement minimization, and generalized displacement control occurred in the range EF. The modified normal flow diverged in point F.

3.10 Problem ten

The truss structure presented in Fig. 20 is subjected to asymmetrical loading. There are three vertical point loads of 2000 N acting on the structure. On the other hand, the truss geometry is also asymmetric. These features lead to a highly nonlinear behavior in the load-deflection curve. This bridge has 33 members and 32 degrees of freedom. The cross-section area of all members is considered to be $A=3 \text{ cm}^2$. The modulus of elasticity is $E=3 \times 10^4 \text{ kN/cm}^2$. Fig. 21 indicates the equilibrium path of this truss for the direction v . Table 20 presents the analysis properties of this structure. Previously, Powell and Simons (1981), Saffari *et al.* (2008) have analyzed this structure.

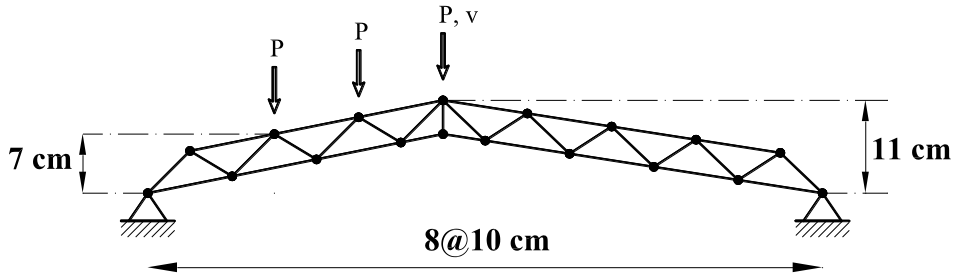


Fig. 20 33-member truss bridge

Table 20 Analysis properties of 33-member truss bridge

Max. of Iteration	Tolerance for Conv.	Arc Length			Target Point	
		Minimum	Increment	Num. of analyses	Load Factor	Displacement
5	1×10^{-5}	5	0.05	300	-	150

Table 21 Numerical results of 33-member truss bridge

Solution Techniques	Number of Analyses	Number of Complete Tracing	Number of Failures	Number of Jumps	Complete Tracing (%)	Steps- Iterations (ratio)
RLM	300	0	300	0	0	Failed
NP	300	170	130	0	56.67	6990- 14707 (2.104)
UNP	300	197	103	0	65.67	6991- 14704 (2.103)
CAL	300	222	78	0	74	6956- 14643 (2.105)
WC	300	0	300	0	0	Failed
RDM	300	200	100	0	66.67	7005- 14818 (2.115)
GDC	300	94	206	0	31.33	6956- 14643 (2.105)
MNF	300	0	300	0	0	Failed

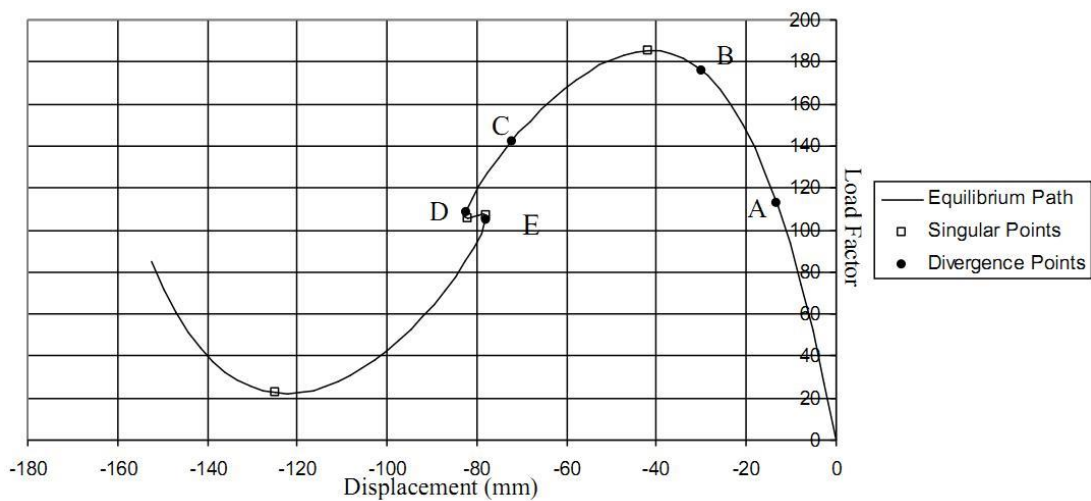


Fig. 21 Equilibrium path of 33-member truss bridge

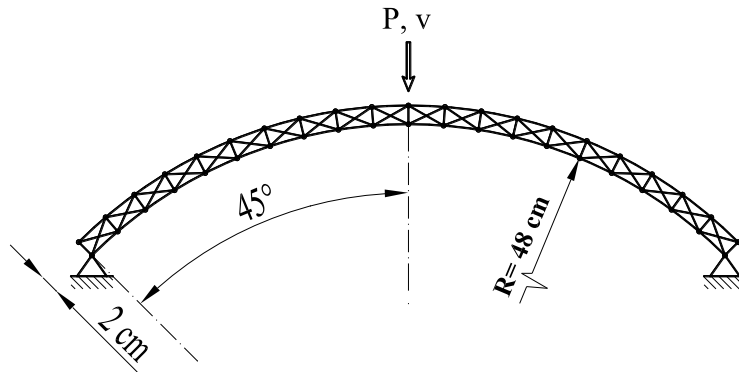


Fig. 22 101-member arc truss

Table 22 Analysis properties of 101-member arc truss

Max. of Iteration	Tolerance for Conv.	Arc Length			Target Point	
		Minimum	Increment	Num. of analyses	Load Factor	Displacement
8	1×10^{-5}	0.01	0.0005	120	200	-

Nonlinear behavior of the present problem has sharp snap-back and snap-through points. Based on the Table 21, the Crisfield cylindrical arc length, the residual displacement minimization, and the updated normal plane are the superior solution techniques. On the other hand, the residual load minimization, work control, and modified normal flow methods did not trace the path completely. To find the number of analysis steps and iterations, the bridge was investigated by utilizing the arc lengths of 5 to 9.45 except for arc length of 8.4 in which some methods diverged. Total number of steps and analysis iterations of the generalized displacement control scheme for the mentioned arc lengths were lesser than that of others.

Referring to Fig. 21, all the analyses of residual load minimization, modified normal flow, and work control methods failed to converge in the ranges of AB, BC, and CD, respectively. Diverged analyses of the normal plane, updated normal plane, cylindrical arc length, and generalized displacement control schemes are situated in point D. 100 analyses of the residual displacement minimization diverged in point E.

3.11 Problem eleven

The arc truss shown in Fig. 22, is subjected to a vertical downward point load of 10 kN at its tip. Arc radius of the truss is $R=48$ cm. Axial rigidity of the members is identical and equal to $EA=50$ MN. The load-deflection curve of this structure for degree of freedom v is given in Fig. 23. Analysis properties of 101-member arc truss are included in Table 22. It is to be noted that this truss has been investigated by other researchers (Crisfield 1997, Hrinda 2007, Thai and Kim 2009).

The obtained number of solution steps and iteration are based on the arc length of 0.016. Among 120 analyses, the residual displacement minimization has the best numerical performance with 93 complete tracing. The residual load minimization and constant work control processes did not trace the path entirely.

Table 23 Numerical results of 101-member arc truss

Solution Techniques	Number of Analyses	Number of Complete Tracing	Number of Failures	Number of Jumps	Complete Tracing (%)	Steps- Iterations (ratio)
RLM	120	0	0	120	0	Failed
NP	120	44	24	52	36.67	144- 150 (1.042)
UNP	120	90	3	27	75	144- 150 (1.042)
CAL	120	62	55	3	51.67	145- 151 (1.041)
WC	120	0	75	45	0	Failed
RDM	120	93	2	25	75.5	145- 150 (1.034)
GDC	120	6	17	97	5	Failed
MNF	120	7	99	14	5.83	Failed

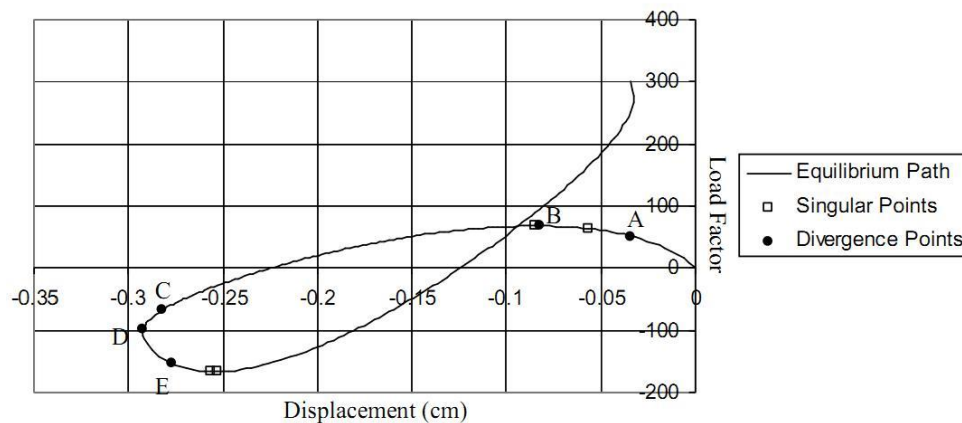


Fig. 23 Equilibrium path of 101-member arc truss

The residual load minimization jumped over the equilibrium path in distance AB. This method returned on the equilibrium path after reaching the first load limit point. Divergent analyses of the work control and normal plane are located in the regions of CD and CE, respectively. The updated normal plane, cylindrical arc length, residual displacement minimization, and modified normal flow tactic also diverged in the range of DE.

3.12 Problem twelve

The truss presented in Fig. 24 has 100 nodes and 260 members. All the members have similar properties. Section diameter of the cylinder is 1000 cm. In fact, section of this cylindrical structure forms a twenty-sided. The cross-section area and the modulus of elasticity of members are $A=650 \text{ cm}^2$ and $E=68950.1 \text{ N/cm}^2$, respectively. All the lower nodes of the truss are clamped. All the top nodes are subjected to downward vertical point load of 1000 N. As it is shown in Fig. 24, there are two-point loads in horizontal direction at the middle nodes symmetrically. Therefore, loading and geometry of the structure is symmetrical. Fig. 25 shows the equilibrium path of the truss for the node under the point load in the middle of the cylinder and in the direction u . Furthermore, the analysis properties of the structure are given in Table 24.

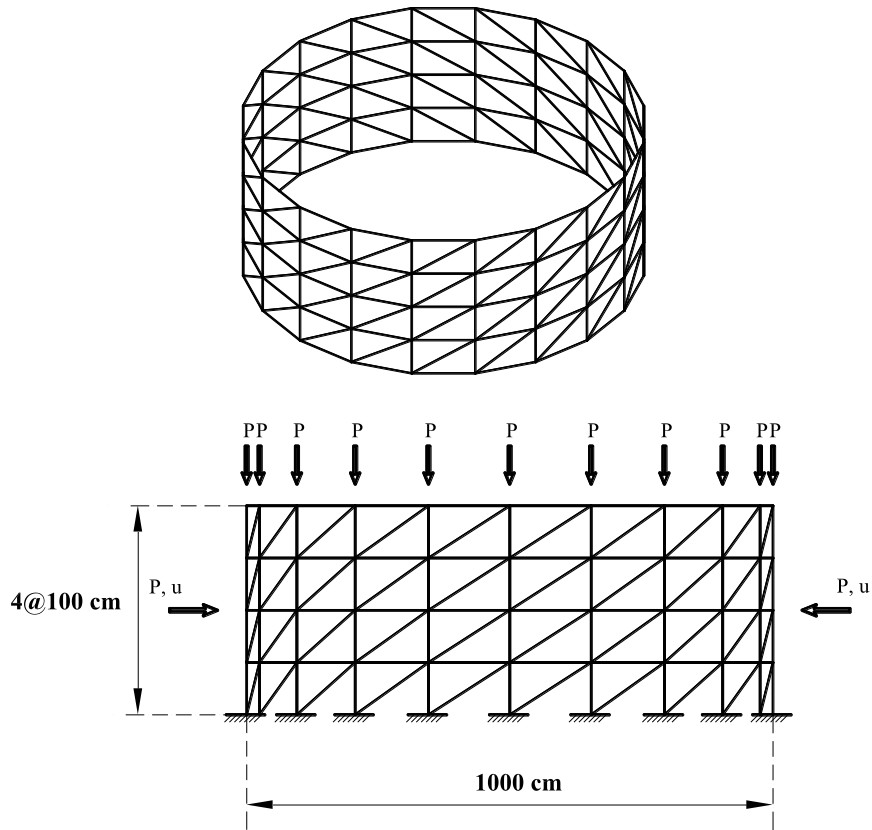


Fig. 24 260-member cylindrical truss

Table 24 Analysis properties of 260-member cylindrical truss

Max. of Iteration	Tolerance for Conv.	Arc Length			Target Point	
		Minimum	Increment	Num. of analyses	Load Factor	Displacement
6	1×10^{-4}	0.01	0.0004	100	-3.24	-0.04

Table 25 Numerical results of 260-member cylindrical truss

Solution Techniques	Number of Analyses	Number of Complete Tracing	Number of Failures	Number of Jumps	Complete Tracing (%)	Steps- Iterations (ratio)
RLM	100	0	88	12	0	Failed
NP	100	61	39	0	61	38- 115 (3.026)
UNP	100	60	40	0	60	38- 115 (3.026)
CAL	100	48	52	0	48	38- 114 (3.000)
WC	100	0	16	0	0	Failed
RDM	100	98	2	0	98	38- 116 (3.053)
GDC	100	68	32	0	68	30- 89 (2.967)
MNF	100	14	86	0	14	Failed

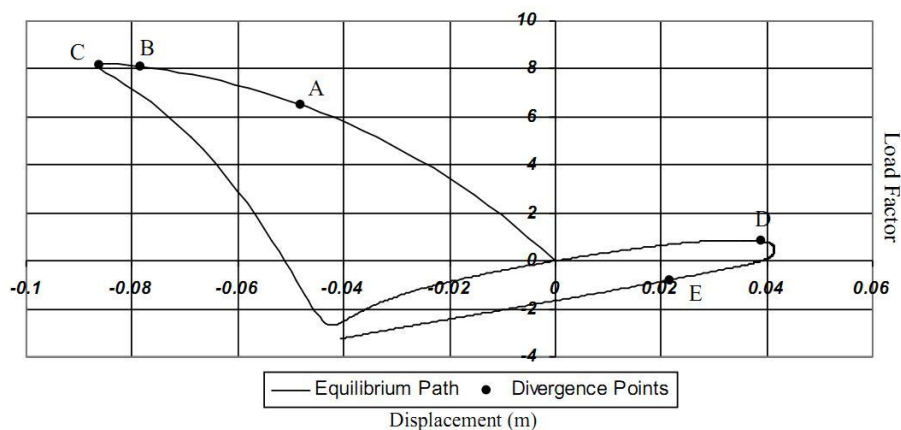


Fig. 25 Equilibrium path of 260-member cylindrical truss

The constant work control and residual load minimization did not successfully trace the load-deflection curve. The residual displacement minimization diverged only in two analyses. The number of solution steps and total number of iterations for the arc length of 0.0275 in the generalized displacement control strategy was lesser than other techniques. Other results are expressed in Table 25.

According to Fig. 25, the constant work control and residual load minimization methods have divergence in the ranges of AB and BC, respectively. The generalized displacement control scheme diverged in points D and E. All diverged solutions of other approaches happened in E.

3.13 Problem thirteen

Dome truss shown in Fig. 26 is generated by cyclic repetitions of the below substructure illustrated in Fig. 26 around the structure axis (Koohestani and Kaveh 2010). This substructure has 9 nodes and 25 members, and central angle of its span is 15 degrees. Based on this data, number of the cyclic repetitions of the substructures will be 24 and the main structure has 216 nodes and 600 truss members. Height of this dome is 7.5 cm and radius of the lowest part is 14 cm. The cross-section area and The modulus of elasticity of members are $A=20 \text{ cm}^2$ and $E=2 \times 10^4 \text{ kN/cm}^2$, respectively. Position of the pinned supports is shown in Fig. 26. The nodes coordinate, and other properties of the substructure are presented in Fig. 26. Loading of this structure is symmetric. There are two downward vertical point loads of 1 MN acting on two opposite nodes at the top of the dome. Fig. 27 shows the load-deflection curve of the structure for the node under the point load and in the vertical direction. In the subsequent problems, evaluating the solution methods with low capability is avoided. The following structures have a large number of degrees of freedom. Therefore, the convergence speed of the techniques will be examined. Analysis properties of single layer circular dome are presented in Table 26.

In this example, comparing of the solution schemes is done by performing 36 analyses for each method. Analysis properties are given in Table 27. The residual displacement minimization with 33 converged analyses and modified normal flow with failure in all analyses, have presented the highest and lowest ability of path tracing, respectively. Numbers of the steps, iterations and

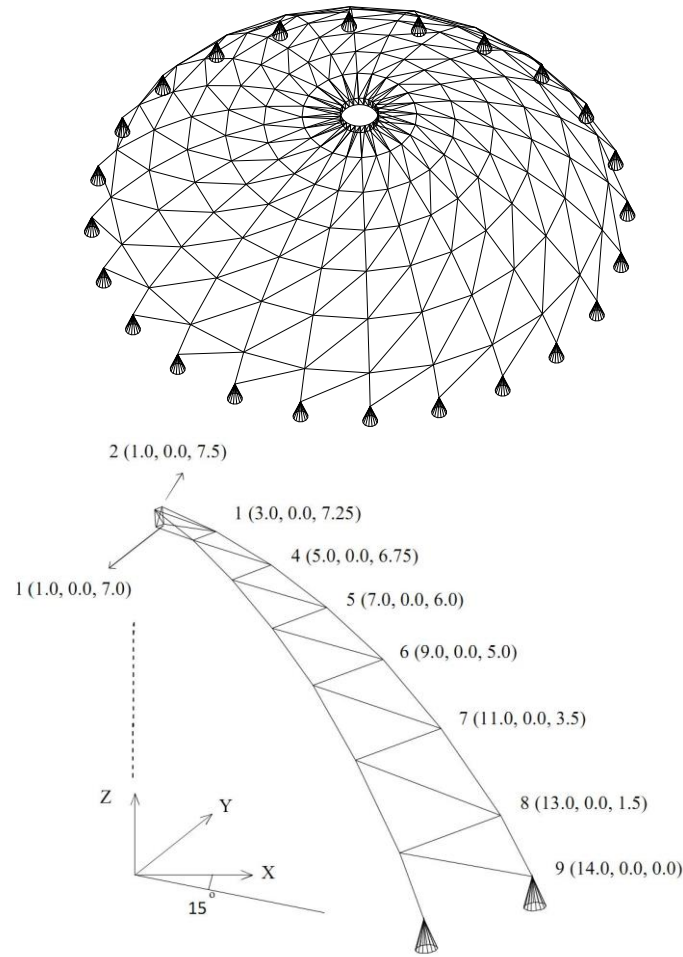


Fig. 26 Single layer circular dome

Table 26 Analysis properties of single layer circular dome

Max. of Iteration	Tolerance for Conv.	Arc Length			Target Point	
		Minimum	Increment	Num. of analyses	Load Factor	Displacement
8	1×10^{-4}	0.01	0.0025	36	-	-0.5

Table 27 Numerical results of single layer circular dome

Solution Techniques	Number of Analyses	Number of Complete Tracing	Number of Failures	Number of Jumps	Complete Tracing (%)	Steps- Iterations (ratio)	Time of Analysis (Seconds)
NP	36	3	33	0	8.33	397- 648 (1.632)	8128
UNP	36	9	27	0	25	397- 644 (1.622)	8105
CAL	36	13	22	1	36.11	399- 648 (1.624)	8160
RDM	36	33	3	0	91.67	402- 663 (1.649)	8290
MNF	36	0	36	0	0	Failed	

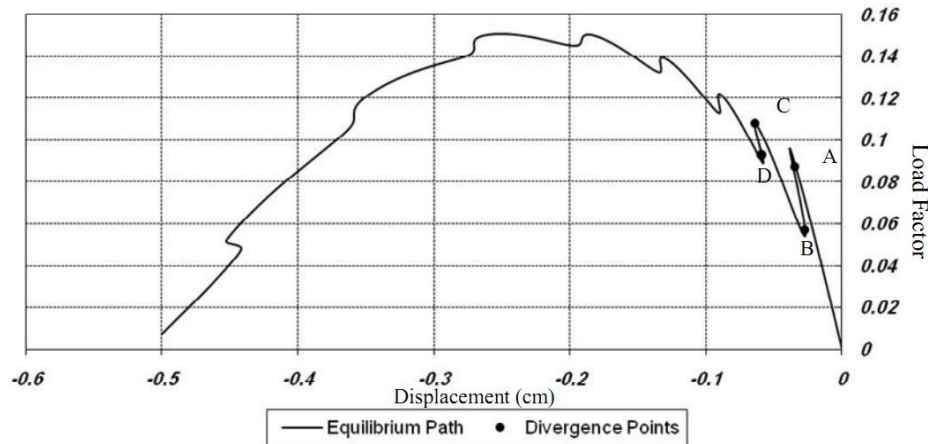


Fig. 27 Equilibrium path of single layer circular dome

running time of the analysis have been shown in Table 27 for the arc length of 0.014. Number of the iterations of the updated normal plane is the least. According to this table, analysis time has a direct relationship with the number of iterations.

Most of the diverged analyses of normal plane, updated normal plane, and cylindrical arc length methods and all the analyses of modified normal flow happened before the first load limit point (A). The Other diverged responses are located as the following: normal plane in points D and C, updated normal plane in points B and D, cylindrical arc length in points B and C, and residual displacement minimization in point D. The performances show that the generalized displacement control technique usually faces difficulties in sharp snap-through points and traverses these points with a lower number of convergent points. As a result, it does not present a truly correct equilibrium path in such points. This solution method diverged in point A.

3.14 Problem fourteen

The structure of Fig. 28 has 390 nodes and 1410 members. The current truss has been obtained by cyclic repetition of substructure shown in Fig. 28 around the Z axis. This substructure has 13 nodes and 47 members. The central angle between one node of a substructure and the corresponding node in the next substructure is 12 degrees. As a result, the dome truss is generated by 30 identical substructures. Maximum (external) and minimum (internal) radius of the two-layer part of the dome are 13 cm and 1 cm, respectively. The structure height reaches 3.88 cm in its crest node. The cross-section area and the modulus of elasticity of all members are $A=10 \text{ cm}^2$ and $E=2 \times 10^4 \text{ kN/cm}^2$, respectively. Positions of the structure supports are shown in Fig. 28. The top node of the dome is subjected to a downward vertical point load of 1000 kN. Table 28 illustrates the analysis properties of the double-layer circular dome. Koohestani and Kaveh (2010) have studied the buckling and free vibration analysis of this dome.

The residual displacement minimization and modified normal flow solution schemes have the best and worst results in tracing the load-deflection curve, respectively. Referring to Table 29, the normal plane and updated normal plane have the lowest number of iterations for the arc length of 0.75. Therefore, they have a shorter running time. It is worth mentioning that the difference

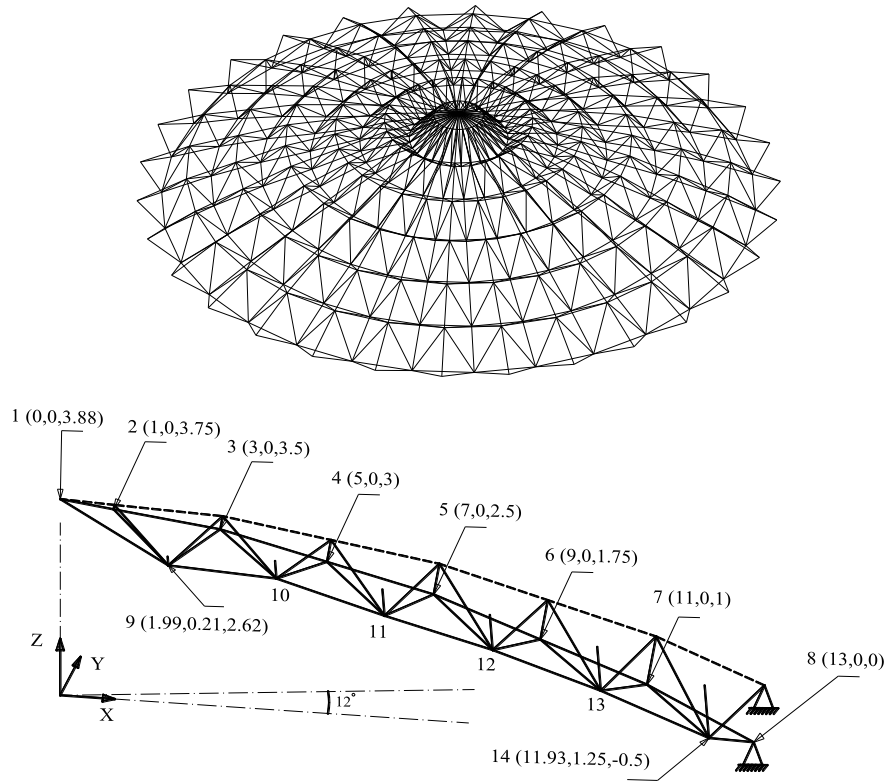


Fig. 28 Double layer circular dome

Table 28 Analysis properties of the double layer circular dome

Max. of Iteration	Tolerance for Conv.	Arc Length			Target Point	
		Minimum	Increment	Num. of analyses	Load Factor	Displacement
7	1×10^{-6}	0.5	0.075	40	-	-6

Table 29 Numerical results of double layer circular dome

Solution Techniques	Number of Analyses	Number of Complete Tracing	Number of Failures	Number of Jumps	Complete Tracing (%)	Steps- Iterations (ratio)	Time of Analysis (Seconds)
NP	40	2	38	0	5	214- 656 (3.065)	25327
UNP	40	7	33	0	17.5	215- 652 (3.033)	25217
CAL	40	14	26	0	35	216- 657 (3.042)	25480
RDM	40	26	14	0	65	218- 668 (3.064)	25797
MNF	40	0	40	0	0	Failed	

between techniques becomes clearer by increasing the arc length size. For instance, the difference in the number of iterations in cylindrical arc length and residual displacement minimization for the arc length of 1.5 reaches to 20 repetitions.

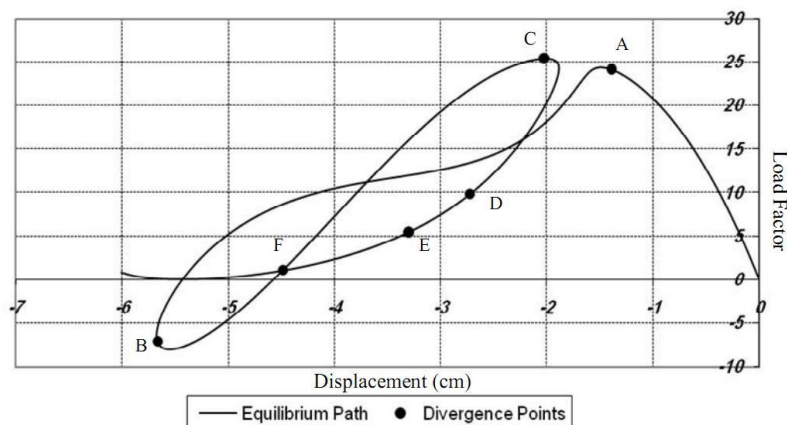


Fig. 29 Equilibrium path of double layer circular dome

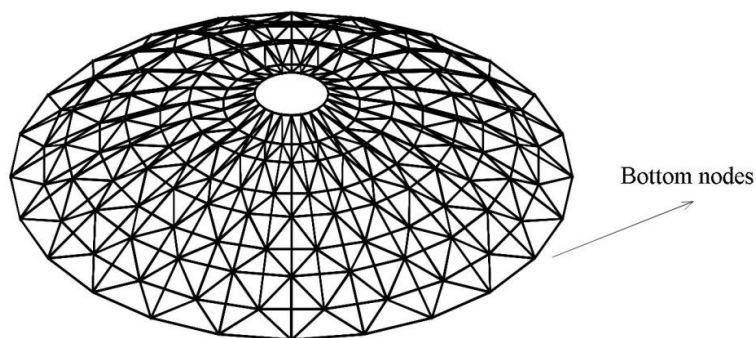


Fig. 30 Double layer canopy dome

Fig. 29 presents the equilibrium path of double layer circular dome under the aforementioned loading. Most of the analyses of normal plane diverged in point C and some of them failed in A and D. The points A, B, and especially C show diverged analyses of the updated normal plane. The cylindrical arc length method diverged in points F, E, and C. The failed analyses of residual displacement minimization approach occurred in C. All the analyses of modified normal flow diverged before load limit point of A.

3.15 Problem fifteen

The dome frame shown in Fig. 30 (Nooshin and Disney 2000) has 216 nodes, 768 frame members, and 1224 degrees of freedom. 24 bottom nodes of the dome are pinned supports. Structure height is 34 cm. The number of rings and elements on the rings are shown in the figure. There are vertical downward point loads of 1000 N acting on all 24 nodes at the top of the dome. The downward displacement of a node under the point load is discussed. All members cross-sections are a circle with area of 0.00785 cm^2 and the modulus of elasticity of $E=200 \times 10^9 \text{ N/cm}^2$. The moment of inertia is equal to $9.817 \times 10^{-6} \text{ cm}^4$. Analysis properties of the double layer canopy dome are included in Table 30.

Table 30 Analysis properties of double layer canopy dome

Max. of Iteration	Tolerance for Conv.	Arc Length			Target Point	
		Minimum	Increment	Num. of analyses	Load Factor	Displacement
8	1×10^{-4}	1	0.25	22	-315	-16.9

Table 31 Numerical results of double layer canopy dome

Solution Techniques	Number of Analyses	Number of Complete Tracing	Number of Failures	Number of Jumps	Complete Tracing (%)	Steps- Iterations (ratio)	Time of Analysis (Seconds)
NP	22	0	22	0	0	Failed	
UNP	22	5	17	0	22.73	166- 369 (2.223)	127190
CAL	22	10	12	0	45.45	167- 372 (2.228)	128173
RDM	22	14	1	7	63.64	168- 378 (2.250)	129835
MNF	22	0	22	0	0	Failed	

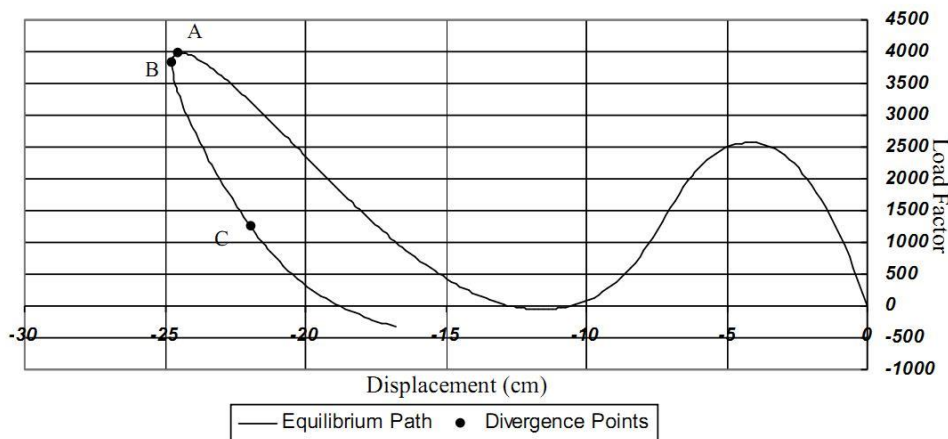


Fig. 31 Equilibrium path of double layer canopy dome

Table 31 indicates the superiority of residual displacement minimization in comparison with other analysis methods. The updated normal plane, cylindrical arc length and normal plane approaches are in the next ranks. The number of iterations and steps for the arc length of 1.75 is given in Table 31. This table illustrates that the updated normal plane has the faster convergence speed.

Fig. 31 presents the equilibrium path of double layer canopy dome. The failed analyses of normal plane, its modified version and cylindrical arc length schemes are located in limit points of B and A. Analyses of the modified normal flow failed in point B. Solution strategy of the residual displacement minimization diverged in B and C.

3.16 Problem sixteen

The shell shown in Fig. 32 is a part of a cylinder. The edges AB and CD are the pinned support, and two other edges are free. The geometrical properties of this structure are illustrated in Fig. 32.

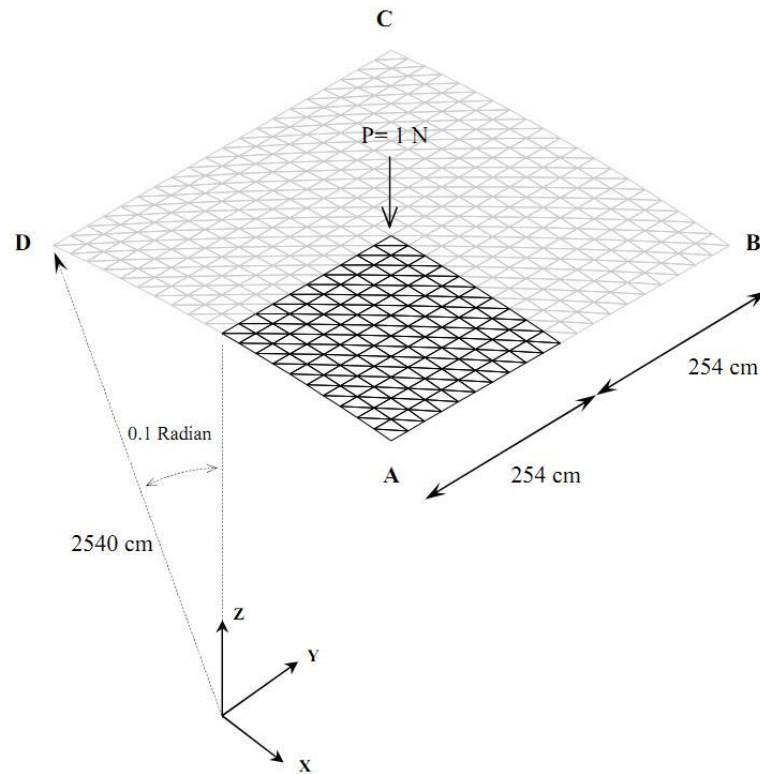


Fig. 32 Cylindrical shell roof

Table 32 Analysis properties of cylindrical shell roof

Max. of Iteration	Tolerance for Conv.	Arc Length			Target Point	
		Minimum	Increment	Num. of analyses	Load Factor	Displacement
10	3×10^{-5}	2	0.2	50	0.2	-

Table 33 Numerical results of cylindrical shell roof

Solution Techniques	Number of Analyses	Number of Complete Tracing	Number of Failures	Number of Jumps	Complete Tracing (%)	Steps- Iterations (ratio)	Time of Analysis (Seconds)
NP	50	50	0	0	100	39- 128 (3.282)	838
UNP	50	16	34	0	32	39- 131 (3.359)	864
CAL	50	18	32	0	36	39- 133 (3.410)	869
RDM	50	50	0	0	100	40- 130 (3.259)	825
MNF	50	33	17	0	66	39- 140 (3.590)	884

The shell is modeled by 800 triangular elements. The modulus of elasticity, Poisson's ratio and the thickness of the shell are $E=3.10275 \text{ N/cm}^2$, $\nu=0.3$ and $t=6.35 \text{ cm}$, respectively. The central node of the shell is subjected to a vertical downward point load of 4 N . Due to symmetry of the structure, one-quarter of the shell is modeled and analyzed. Table 32 shows the analysis properties

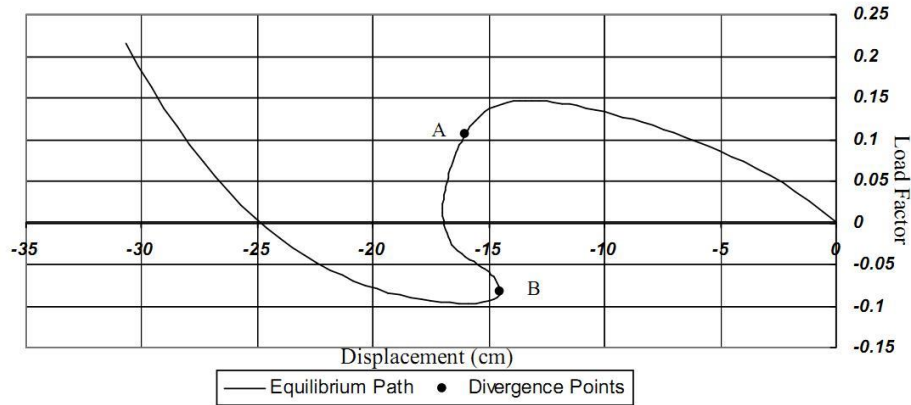


Fig. 33 Equilibrium path of cylindrical shell roof

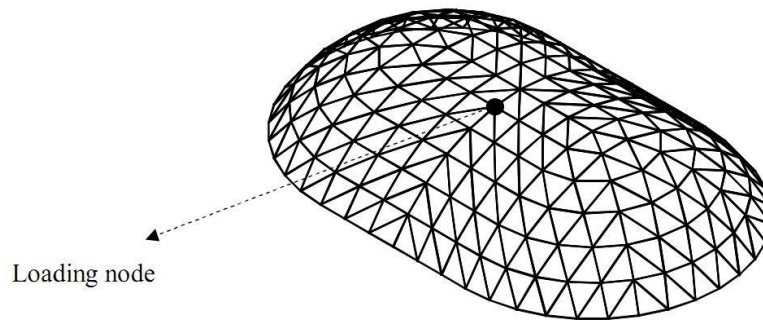


Fig. 34 Dome shell

of this shell. Because of snapping behavior, many researchers have studied this shell (Surana 1982, Surana 1983, Lee and Kanok-Numkulchai 1998, Sze and Zheng 1999, Sze and Chan 2002, Sze and Zheng 2002, Sze *et al.* 2004).

Referring to Table 33 approaches of normal plane and residual displacement minimization have traced the equilibrium path completely. Moreover, these techniques have the minimum number of iterations and analysis time for the arc length of 6.4.

Fig. 33 shows the equilibrium path of this structure for the node under the point load and in the vertical direction. Updated normal plane and cylindrical arc length failed in point A, and modified normal flow diverged in B.

3.17 Problem seventeen

Fig. 34 (Nooshin and Disney 2000) shows a dome with a height of 10 cm and width of 35 cm. All the nodes in the lowest part of the dome are clamped supports. A vertical downward point load of 1000 N is acting on the black point indicated in Fig. 34. The modulus of elasticity, Poisson's ratio and the thickness of the shell are $E=2 \times 10^{11} \text{ N/cm}^2$, $\nu=0.3$ and $t=0.02 \text{ cm}$, respectively. This structure is modeled with 360 triangular elements. Analysis properties of the dome shell are presented in Table 34.

Table 34 Analysis properties of dome shell

Max. of Iteration	Tolerance for Conv.	Arc Length			Target Point	
		Minimum	Increment	Num. of analyses	Load Factor	Displacement
20	1×10^{-4}	0.02	0.001	40	317	-0.36

Table 35 Numerical results of dome shell

Solution Techniques	Number of Analyses	Number of Complete Tracing	Number of Failures	Number of Jumps	Complete Tracing (%)	Steps- Iterations (ratio)	Time of Analysis (Seconds)
NP	40	25	9	6	62.5	20- 111 (5.55)	1497
UNP	40	0	40	0	0	Failed	
CAL	40	0	40	0	0	Failed	
RDM	40	29	11	0	72.5	22- 110 (5)	1570
MNF	40	18	22	0	45	20- 122 (6.1)	1698

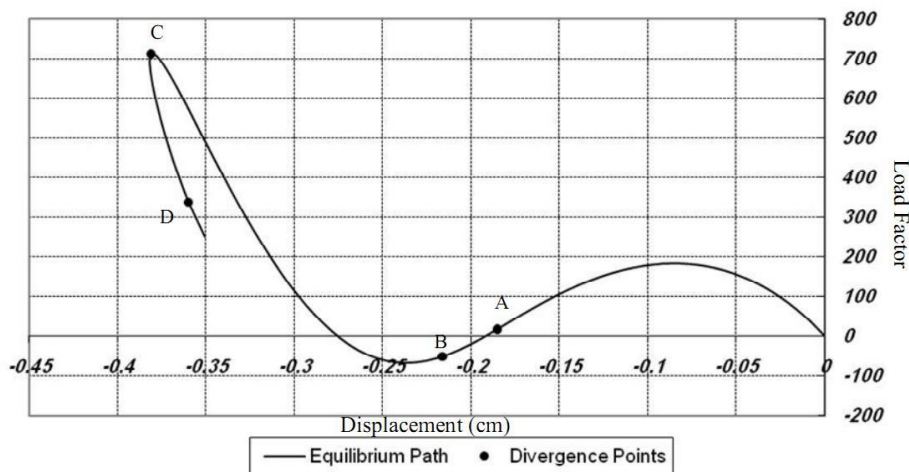


Fig. 35 Equilibrium path of dome shell

Based on Table 35, the methods of updated normal plane and cylindrical arc length don't achieve a complete trace. The residual displacement minimization method has the highest convergence ability. The scheme of normal plane has a shorter running time in comparison with the residual displacement minimization and modified normal flow tactics. It is to be noted that, the arc length of 0.045 was employed for determining the number of steps, iterations, and also the analysis time.

Fig. 35 shows the equilibrium path of dome shell for the node under the point load and in the downward direction. The failed analyses of updated normal plane and cylindrical arc length procedures occurred in the range of AB. The diverged analyses of normal plane technique are located in point C. Furthermore, the points C and D show the situation of diverged responses for the residual displacement minimization. Point C also specifies the divergence location of the modified normal flow and generalized displacement control algorithms.

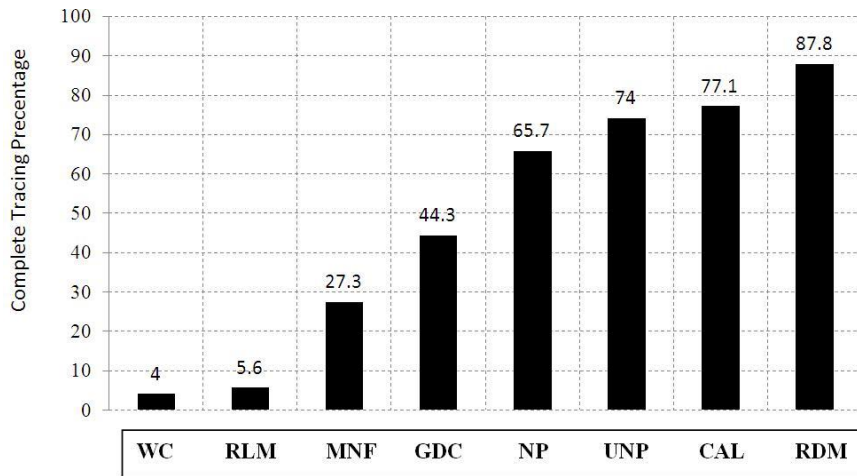


Fig. 36 Total results of tracing the equilibrium path completely

4. Conclusions

In this article, a comprehensive and detailed assessment of nonlinear structural solution techniques was carried out. For this purpose, 17 problems with geometrical nonlinear behavior were analyzed more than 12500 times. Approaches like residual load minimization, normal plane, updated normal plane, cylindrical arc length, work control, residual displacement minimization, generalized displacement control, modified normal flow methods were broadly compared in this study. Some of the superiorities of the present investigation in comparison with other similar researches will be given in the following:

1-Most of the significant and well known nonlinear solution strategies were studied comprehensively.

2-The criteria employed in this study made the findings of comparison procedure very clear and reliable. These standards include the power and speed of convergence, ability to pass the load limit and snap-back points and total number of analysis iterations and steps.

3-Utilizing a large number of benchmark problems and variety of structural nonlinear behavior increase the reliability of the comparison procedure.

Basic differences in the constraint equations belong to the solution schemes lead to different results. For example, Crisfield arc length method returns to the equilibrium path by the geometrical constraint, while the displacement minimization algorithm acts based on the residual displacement. Accordingly, by solving several different problems, an accurate evaluation will be obtained. Finally, the authors present the total results of completely traced equilibrium path, as illustrated in Fig. 36.

Bar graph of Fig. 36 demonstrates the total results of completely traced paths. According to the findings, solution scheme of the residual displacement minimization has the best convergence ability by tracing 87.8% of the equilibrium paths in more than 12500 analyses. The outcomes indicated that this strategy is highly capable in tracing the structural equilibrium paths by small and large load increments. Load limit points can be easily passed by this method. The constant work control and residual load minimization methods have the weakest solution ability because of failing in traversing load limit points and snap-back points, respectively. The cylindrical arc

length, updated normal plane and normal plane techniques also have acceptable results in tracing structural equilibrium path.

Generally, generalized displacement control method traces a longer path with a specific load increment than the other techniques, although this approach is not very robust in tracing all kinds of equilibrium paths. Furthermore, this solution scheme has a high convergence speed and achieves the target point with lower analysis steps. The results denote the direct relationship between the total number of analysis iterations and the computer running time. In other words, solutions with fewer numbers of iterations have higher convergence speed. Also, normal plane and updated normal plane strategies mostly converged with the lesser number of iterations and, consequently, higher analysis speed among the other methods. In some cases, normal plane and updated normal plane jump over the main path due to their returning condition, which happens more than other processes. Normal plane, updated normal plane, and generalized displacement control techniques do not have a high capability to pass sharp snap-back points, especially in large load increments. These approaches usually do not present an accurate path in the vicinity of mentioned points, and they go to the next step by jumping over these points.

Based on the author's extensive numerical experiences, this study introduces the following ranks for the analysis capabilities of nonlinear solution techniques:

- 1- Residual Displacement Minimization.
- 2- Cylindrical Arc Length.
- 3- Updated Normal Plane.
- 4- Normal Plane.

References

- Bathe, K.J. Dvorkin, E.N. (1983), "On the automatic solution of nonlinear finite element equations", *Comput. Struct.*, 871-879.
- Bergan, P.G., Horrigmoe, G., Bråkeland, B. and Søreide, T.H. (1978), "Solution techniques for non-linear finite element problems", *Int. J. Num. Meth. Eng.*, **12**(11), 1677-1696.
- Cardona, A. and Huespe, A. (1998), "Continuation methods for tracing the equilibrium path in flexible mechanism analysis", *Eng. Comput.*, **15**(2), 190-220.
- Chen, H. and Blandford, G.E. (1993), "Work-increment-control method for non-linear analysis", *Int. J. Num. Meth. Eng.*, **36**(6), 909-930.
- Clarke, M.J. and Hancock, G.J. (1990), "A study of incremental-iterative strategies for non-linear analyses", *Int. J. Num. Meth. Eng.*, **29**(7), 1365-1391.
- Crisfield, M.A. (1997), *Non-Linear Finite Element Analysis of Solids and Structures*, Volume 2 Advanced Topics, John Wiley & Sons.
- Eduardo Nobre Lages, G.H.P. (1999), "Nonlinear finite element analysis using an Object-Oriented Philosophy-Application to Beam Elements and to the Cosserat Continuum", *Eng. Comput.*, **15**, 73-89.
- Feenstra, P.H. and Schellekens, J.C.J. (1991), "Self-adaptive solution algorithm for a constrained Newton-Raphson method", Delft University of Technology, Department of Civil Engineering, Stevin laboratory-Mechanics & Structures Division, Netherlands.
- Geers, M.G.D. (1999), "Enhanced solution control for physically and geometrically non-linear problems. Part II-comparative performance analysis", *Int. J. Num. Meth. Eng.*, **46**(2), 205-230.
- Gorgun, H. and Yilmaz, S. (2012), "Geometrically nonlinear analysis of plane frames with semi-rigid connections accounting for shear deformations", *Struct. Eng. Mech.*, **44**(4), 539-569.
- Harrison, H. (1983), "Elastic post-buckling response of plane frames", *Instability and Plastic Collapse of Steel Structures*, Ed. Morris, L.J., Granada, 56-65.

- Huang, B.Z. and Atluri, S.N. (1995), "A simple method to follow post-buckling paths in finite element analysis", *Comput. Struct.*, **57**(3), 477-489.
- Hrinda, G.A. (2007), "Geometrically nonlinear static analysis of 3D trusses using the arc-length method", *Computational Methods and Experimental Measurements XIII*, Prague, Czech Republic, 243-252.
- Kim, T.H., Cheon, J.H. and Shin, H.M. (2009), "Evaluation of behavior and strength of prestressed concrete deep beams using nonlinear analysis", *Comput. Concrete*, **9**(1), 63-79.
- Koohestani, K. and Kaveh, A. (2010), "Efficient buckling and free vibration analysis of cyclically repeated space truss structures", *Finite Elem. Anal. Des.*, **46**(10), 943-948.
- Kuo Mo Hsiao and Fang Yu Hou (1987), "Nonlinear finite element analysis of elastic frames", *Comput. Struct.*, **26**(4), 693-701.
- Lee, S., Manuel, F.S. and Rossow, E.C. (1968), "Large deflections and stability of elastic frame", *J. Eng. Mech. Div.*, **94**(2), 521-548.
- Lee, S.J. and Kanok-Nukulchai, W. (1998), "A nine-node assumed strain finite element for large-deformation analysis of laminated shells", *Int. J. Num. Meth. Eng.*, **42**(5), 777-798.
- Loganathan, S. (1989), "Geometric and material nonlinear behaviour of space frame structures", Ph.D. Thesis, The University of Queensland.
- Meek, J.L. and Loganathan, S. (1989), "Large displacement analysis of space-frame structures", *Comput. Meth. Appl. Mech. Eng.*, **72**(1), 57-75.
- Meek, J.L. and Xue, Q. (1998), "A study on the instability problem for 3D frames", *Comput. Meth. Appl. Mech. Eng.*, **158**(3-4), 235-254.
- Noor, A.K. and Peters, J.M. (1983), "Instability analysis of space trusses", *Comput. Meth. Appl. Mech. Eng.*, **40**(2), 199-218.
- Nooshin, H. and Disney P.L. (2000), "Formex configuration processing I", *Int. J. Space Struct.*, **15**(1), 1-52.
- Powell, G. and Simons, J. (1981), "Improved iteration strategy for nonlinear structures", *Int. J. Num. Meth. Eng.*, **17**(10), 1455-1467.
- Ramesh, G. and Krishnamoorthy, C.S. (1994), "Inelastic post-buckling analysis of truss structures by dynamic relaxation method", *Int. J. Num. Meth. Eng.*, **37**(21), 3633-3657.
- Rezaiee-Pajand, M., Tatar, M. and Moghaddasie, B. (2009), "Some geometrical bases for incremental-iterative methods", *Int. J. Eng., Tran. B: Appl.*, **22**(3), 245-256.
- Saffari, H., Fadaee, M.J. and Tabatabaei, R. (2008), "Nonlinear analysis of space trusses using modified normal flow algorithm", *J. Struct. Eng.*, **134**(6), 998-1005.
- Schellekens, J.C.J., Feenstra, P.H. and de Borst, R. (1992), "A self-adaptive load estimator based on strain energy", *Computational Plasticity, Fundamentals and Applications*, Eds. Owen, D.R.J., Onate, E. and Hinton, E., CIMNE, Barcelona, Pineridge Press, 187-198.
- Schweizerhof, K.H. and Wriggers, P. (1986), "Consistent linearization for path following methods in nonlinear FE analysis", *Comput. Meth. Appl. Mech. Eng.*, **59**(3), 261-279.
- Simo, J.C. and Vu-Quoc, L. (1986), "A three-dimensional finite-strain rod model. part II: Computational aspects", *Comput. Meth. Appl. Mech. Eng.*, **58**(1), 79-116.
- Surana, K.S. (1982), "Geometrically non-linear formulation for the three dimensional solid-shell transition finite elements", *Comput. Struct.*, **15**(5), 549-566.
- Surana, K.S. (1983), "Geometrically nonlinear formulation for the curved shell elements", *Int. J. Num. Meth. Eng.*, **19**(4), 581-615.
- Sze, K.Y., Chan, W.K. and Pian, T.H.H. (2002), "An eight-node hybrid-stress solid-shell element for geometric nonlinear analysis of elastic shells", *Int. J. Num. Meth. Eng.*, **55**, 853-878.
- Sze, K.Y. and Zheng, S.J. (1999), "A hybrid stress nine-node degenerated shell element for geometric nonlinear analysis", *Comput. Mech.*, **23**(5), 448-456.
- Sze, K.Y. and Zheng, S.J. (2002), "A stabilized hybrid-stress solid element for geometrically nonlinear homogeneous and laminated shell analyses", *Comput. Meth. Appl. Mech. Eng.*, **191**(17-18), 1945-1966.
- Thai, H.T. and Kim, S.E. (2009), "Large deflection inelastic analysis of space trusses using generalized displacement control method", *J. Constr. Steel Res.*, **65**(10-11), 1987-1994.
- Williams, F.W. (1964), "An approach to the non-linear behaviour of the members of a rigid jointed plane

- framework with finite deflections”, *Q. J. Mech. Appl. Math.*, **17**(4), 451-469.
- Wood, R.D. and Zienkiewicz, O.C. (1977), “Geometrically nonlinear finite element analysis of beams, frames, arches and axisymmetric shells”, *Comput. Struct.*, **7**(6), 725-735.
- Xu, T., Xiang, T., Zhao, R. and Zhan, Y. (2010), “Nonlinear finite element analysis of circular concrete-filled steel tube structures”, *Struct. Eng. Mech.*, **35**(3), 315-333.
- Yang, Y.B. and Kuo, S.R. (1994), *Theory and Analysis of Nonlinear Framed Structures*, Singapore, Prentice Hall.
- Yang, Y.B. and Shieh, M.S. (1990), “Solution method for nonlinear problems with multiple critical points”, *AIAA J.*, **28**(12), 2110-2116.
- Yang, Y.B., Yang, C.T., Chang, T.P. and Chang, P.K. (1997), “Effects of member buckling and yielding on ultimate strengths of space trusses”, *Eng. Struct.*, **19**(2), 179-191.